U.S. DEPARTMENT OF THE INTERIOR

U.S. GEOLOGICAL SURVEY

Re-examination of rock geochemistry in the Copper Canyon area, Lander County, Nevada

by

Boris B. Kotlyar, Ted G. Theodore, and Robert C. Jachens

Menlo Park, California 94025

Open-File Report 95–816

1995

RE-EXAMINATION OF ROCK GEOCHEMISTRY IN THE COPPER CANYON AREA, LANDER COUNTY, NEVADA

by

Boris B. Kotlyar, Ted G. Theodore, and Robert C. Jachens

Abstract

Re-examination of rock geochemistry from an approximately 16–km^2 area at Copper Canyon, Nev., reveals a number of striking relations of zoned metal distributions that were previously only faintly recognizable. Geochemical data from a 2,710–sample database were interpolated to 100–m- and 500–m-wide cells and filtered of short wavelength changes among elements. The samples were analyzed in 1968 prior to subsequent discovery of as many as 10 deposits in a skarn-related porphyry copper environment that includes the world-class Fortitude gold skarn, which produced approximately 2 million oz Au between 1984 and 1993. The Copper Canyon area is inferred to have included a geologic resource of as much as 5 million oz Au prior to the startup of major mining operations. Machine-contoured plots for Au, Ag, Sn, As, Hg, and Pb all show various degrees of development of a semi-annular ring or hook-shaped pattern of elevated abundances around four major ore bodies (Lower Fortitude, Upper Fortitude, Phoenix, and West ore body) which are present north of the late Eocene and (or) early Oligocene altered granodiorite of Copper Canyon. The most striking of these plots is that for mercury. Partly on the basis of these plots, we suggest that all these metals were introduced into various rock units and faults as part of a single protracted mineralizing event, in places and at times associated with development of prograde skarn and potassic alteration assemblages, as well as with all of the retrograde mineral assemblages prevalent in a porphyry copper system. Although mercury is not a metal commonly considered to be associated closely with orebodies in a porphyry copper environment, it appears incontrovertible that mercury forms a significant halo or fringing anomaly to some of the largest skarn-hosted Au–Ag–Cu orebodies north of the altered granodiorite of Copper Canyon. Some of the highest concentrations of mercury coincide with Pb–Zn–Ag polymetallic veins peripheral to the skarns.

Although plots using an elevated filtering factor (z equals 500 m) are extremely generalized, they illustrate well many aspects of lithogeochemistry at Copper Canyon. Their usage could have applications in regional stream-sediment geochemical surveys and geoenvironmental studies. A contoured plot for mercury utilizing z equals 500 m reveals that the semi-annular ring of anomalies north of the altered granodiorite of Copper Canyon coalesces into a broad anomaly centered just north of the Fortitude deposit. There are additional indications that elevated mercury abundances continue to the north beyond the area, and possibly continue to the northeast. In the

southern part of the area, the contoured plot for mercury also shows a progressive increase in mercury concentrations that appears to extend beyond the southern boundary of the area. Nonetheless, the two mercury anomalies appear to define a "dumbbell"-shaped pattern that has its northern part much more strongly developed than the southern one. This relation for mercury is consistent with more deeply eroded parts of the geochemical system being present on the south, as are the patterns for some of the other metals examined, because the southern part of the area is at a much lower elevation than the northern part.

Introduction

As part of recent ongoing cooperative studies with private industry of rock geochemistry as it relates to geoenvironmental ore-deposit models in the skarn environment (Hammarstrom and others, 1995a, b, c), a large rock geochemistry database for the Copper Canyon area, Nev., (Theodore, 1970) was re-examined (fig. 1). The Copper Canyon area is in north-central Nevada, and in the southern part of the Battle Mountain Mining District (Roberts and Arnold, 1965). The Copper Canyon area is host to a number of large epigenetic orebodies—as many as ten, which were not known and, of course, were not drilled out at the time the area was sampled by the U.S. Geological Survey in 1968. As a result, disturbance of the original ground surface by mining activities at Copper Canyon was restricted to the immediate area of only one of the large orebodies—the East ore body. In addition, there are a number of small polymetallic vein and skarn occurrences in this approximately 16–km^2 area that had some minor production of base and precious metals as early as the 1860s. A gold placer operation produced approximately 100,000 oz Au between 1917 and 1955 from the alluvial fan at the mouth of Copper Canyon (Roberts and Arnold, 1965; Doebrich and others, 1995). Although the area historically was known for its large production of copper from 1967 to about 1978, since that time Copper Canyon has become one of the largest producers of gold in north-central Nevada. Approximately 5 million oz Au, including past production and projected future geologic resources, have been outlined to date (1995) in the Copper Canyon area (P.R. Wotruba, oral commun., 1994; see also, Doebrich and others, 1995).

The purpose of this report is to describe additional insights into the process of mineralization, particularly with respect to metal zoning, that have been gained by application of numerous advances in geochemical investigations over the intervening 28 years—including many reported in the geochemical literature from Russia (see also, Beus and Grigorian, 1977)—since the original geochemical study was conducted at Copper Canyon. Much additional information, recently gathered from Copper Canyon, results from modern methods of data processing of geochemical data that can be combined with exploration hindsight, and allows us to examine geochemical relations in rock exposures from the perspective of subsequent discoveries of large numbers of ore bodies at depth. For example, geochemical data from bedrock around the world-class Fortitude gold skarn (Wotruba and others, 1986) suggests the presence of some halos of

certain elements. These relations can then be used for predictive purposes elsewhere in the mining district or in other mining districts that contain similar geology and similar deposit types. The main intent of the present report is to show how individual anomalies of certain introduced elements, in both mineralized structures and rocks of the host formations, when composited areally using standard geophysical gridding and filtering procedures, exhibit zoned distributions of geochemical domains that are consistent with thermodynamic theories of element migration, and that these zonal distributions may have predictive value. Many of these zoned distributions become readily apparent when examined by the gridding and filtering procedures in contrast to their subtle presence when examined by other means.

Acknowledgments

We wish again to gratefully acknowledge the large numbers of analysts from the Branch of Geochemistry of the U.S. Geological Survey, who, at times, labored now close to 30 years ago under difficult field conditions to complete the number of analyses generated by geologic investigations in the Battle Mountain Mining District. Their active participation, though long past, continues to form the basis for investigations that, we believe, have significant merit. The continued interest of management of Battle Mountain Exploration Co.—particularly Patrick R. Wotruba and Michael Broch— in our investigations at Copper Canyon has provided us a scientifically healthy opportunity to exchange numerous ideas that sometimes failed the "outcrop test" and sent us back to the drawing board. Regardless, we appreciate the access to data that they have provided to us over the years, because without this access we could not have generated viable ideas.

Geology of Copper Canyon Area

The Copper Canyon area includes two major allochthonous terranes—one accreted during the late Devonian and (or) early Mississippian Antler orogeny, and the other during the latest Permian and (or) early Triassic Sonoma orogeny (Roberts and others, 1958; Silberling and Roberts, 1962; Roberts, 1964). The former accreted terrane includes the allochthon of the Roberts Mountains thrust, which, at Copper Canyon, is made up of the Upper Cambrian Harmony Formation and the Devonian Scott Canyon Formation (Roberts, 1964; Theodore and Blake, 1975, ,1978; Doebrich, 1995; Doebrich and others, 1995). The latter accreted terrane is made up of the upper plate of the Golconda thrust, which at Copper Canyon includes strata belonging to lithotectonic unit 1 of Murchey (1990) of the Mississippian, Pennsylvanian, and Permian Havallah sequence (Doebrich, 1995). These rocks formerly were assigned to the Pennsylvanian (?) Pumpernickel Formation of Roberts (1964). In addition, an intervening block of autochonous rock is present between the two accreted terranes, and this block (Pennsylvanian and Permian Antler sequence, fig. 1*A*) belongs to the overlap assemblage of Roberts (1964). The Antler

sequence includes the Middle Pennsylvanian Battle Formation, the Pennsylvanian and Permian Antler Peak Limestone, and the Permian Edna Mountain Formation (Theodore and Blake, 1975; Doebrich, 1995). At Copper Canyon, the Antler sequence is present as a number of north-south elongate, discontinous lenses that dip to the west, and that are bounded along their western margins by a number of west-dipping, high angle, Tertiary normal faults (fig.1A).

A small altered granodiorite pluton, emplaced during late Eocene and (or) early Oligocene (38–40 Ma, Theodore and others, 1973), intruded the major tectonic terranes at Copper Canyon (fig.1*A*), and it is the near-surface paleo-expression of a shallow-seated magmatic hydrothermal system that was responsible for the porphyry copper, porphyry copper skarn-related, gold skarn, distal disseminated, and small polymetallic vein deposits that are present in the area (Roberts and arnold, 1965; Theodore and Blake, 1975, 1978). A broad halo of hornfels, including pyrite and pyrrhotite, surrounds the altered granodiorite, and extends as much as 1.5 km northeast of the altered granodiorite.

Two packages of rock contributed significantly to development of major ore bodies at Copper Canyon. The chemically receptive rocks of the Antler sequence are important from the standpoint of mineralization because they host the bulk of the gold and copper ores at Copper Canyon. The Lower Fortitude gold skarn, formed mostly in the Antler Peak Limestone (fig. 1*A*; see also, Wotruba and others, 1988; Myers, 1994), is perhaps the most important of the gold ore bodies in the area—it produced approximately 1.75 million oz Au between 1984 and 1993 (Doebrich and others, 1995). Currently (1995), mining operations at Copper Canyon are focused at the Midas pit—this is an oxidized gold skarn that includes abundant copper in its northern proximal parts and abundant lead and zinc in its southern distal parts near the mouth of Copper Canyon (fig.1*A*). The second package of rocks that played a key role in the mineralization process is the Havallah sequence and its relatively impervious and nonreactive, thick sequences of argillite and chert. These rocks acted as a barrier to flow of ascending mineralizing fluids circulating in the general area of the altered granodiorite, and the argillite and chert effectively channeled these fluids laterally into some of the receptive carbonate strata where the best ores eventually were formed. Nonetheless, some penetration of mineralizing fluids into the relatively impervious argillite and chert must have occurred as exemplified by the presence of a number of small vein deposits and occurrences in these rocks (fig. 1A), and by moderate positive factor-analysis loadings for the mineralizing suite of elements (Cu, Au, Ag, As, Pb, Zn, As, and several others) on the analyzed argillite and chert (B.B. Kotlyar and T.G. Theodore, unpub. data, 1995).

The Copper Canyon area, as well as other Tertiary loci of mineralization elsewhere in the Battle Mountain Mining District, is located in a broad domain that marks the intersection of two fault zones (Doebrich and others, 1995). Both of these zones, one trending north-south and the

other trending northwest, probably developed over a relatively short time span in the Tertiary from some time prior to 40 Ma to approximately 31 Ma.

Previous geochemical studies

As part of the U.S. Geological Survey's Heavy Metals Program in the late 1960s, 2,927 rock samples were collected and analyzed from the Copper Canyon area (Theodore, 1970; Theodore and Blake, 1975). The samples were analyzed for 30 elements by emission spectrographic methods (Grimes and Marranzino, 1968), and for gold and mercury by atomic absorption and a cold-vapor atomic absorption procedure, respectively (Haffty and others, 1977; Wilson and others, 1987). A report by Theodore (1969) shows surface distribution of 20 elements at the respective sampling sites, classified according to numerical intervals determined largely from breaks in elemental distributions noted in histograms prepared from data obtained from the northern third of the Copper Canyon area. The northern part of the Copper Canyon area shows minimal epigenetic introduction of many metals across wide areas because it is largely beyond the area converted to hornfels and sulfidized around the altered granodiorite. Figure 2, the geochemical spot map for mercury reproduced from Theodore (1969), exemplifies these data plots.

Various aspects of rock geochemistry at Copper Canyon also are described by Theodore and Nash (1973), Theodore and Blake (1975, 1978), and Theodore and others (1986). However, these early geochemical studies emphasized presence of elevated metal concentrations along mineralized structures and the apparent channelling of mineralizing fluids along many normal faults that predated mineralization in the area. Much of the rock between these mineralized faults does not contain concentrations of metals similar in magnitude to those present along the mineralized faults. There are two general levels of metal concentration in the widely sulfidized part of the Copper Canyon area: extremely elevated metal concentrations along mineralized faults (including fault gouge, fault breccia, oxidized sulfide minerals, and vein minerals), and somewhat lower absolute levels of the same suite of metals in altered rocks away from the mineralized faults. Nonetheless, the latter are significantly anomalous when compared to crustal abundances. Again, it should be emphasized that the only significant disturbance of the ground at the time of sampling was in the immediate area of the East ore body (figs.1, 2), which is a copper-gold-silver replacement orebody formed in the Battle and Harmony Formations, and which is notable for its potassic alteration assemblages and absence of skarn assemblages (Theodore and Blake, 1975).

For comparative purposes, the distributions of five elements at Copper Canyon (copper, lead, mercury, arsenic, and cadium; fig. 1*B–F*) are shown. These figures were prepared from the plots of Theodore (1969) by visually outlining areas that appear to have elemental abundances of approximately the same magnitude, and then drawing contours by hand. The most widespread

elevated concentration of the epigenetic suite of metals associated with mineralization at Copper Canyon is copper (fig.1*B*). A broad equant area of elevated copper concentrations (>700 ppm Cu) extends from the general area of the East ore body west and southwest to the main drainage through Copper Canyon. Most copper in this area appears to result from supergene downslope migration of copper from the topographically high East orebody. Chalcopyrite-pyrrhotite assemblages were abundant in the potassic alteration assemblages in the East ore body (Theodore and Blake, 1975). Furthermore, the ridge where the East orebody was located—now removed by the open pit mining operations—was locally known as "Pyrrhotite Ridge." Abundant copper is present in clay-altered plagioclase phenocrysts, commonly pale apple green in outcrop, of the altered granodiorite of Copper Canyon. Much of the exposed altered granodiorite has near-surface concentrations of greater than 10,000 parts per million (ppm) Cu; however, such elevated abundances of copper are tightly constrained to an exceedingly thin volume of rock that follows topography. Cadmium, in contrast to copper, shows a sparse distribution over all the area, and the highest contents of cadmium coincide with a number of Pb–Zn–Ag–(Au)-mineralized faults near the northern margin of the Fortitude deposit (fig. 1*F*). This part of the underlying Fortitude deposit contains relatively high concentrations of sphalerite. The distribution of mercury appears to have a diffuse spotty concentration generally in the central part of the Copper Canyon area. We will return again to implications of its distribution when evaluated by other methods (fig. 1*D*). The most widespread concentration of mercury contents in the 0.2 to 1.0 ppm range is in an area straddling the Copper Canyon drainage in the general area of a mineralized fault strand of the Copper Canyon fault system that passes through a small vein deposit at the Sonderman prospects (see also, Theodore and Blake, 1975).

Data base

From the original data base that contained 2,927 analyzed samples (Theodore, 1970), a data base of 2,710 samples was extracted and verified with regards to sample locations, rock types, and element contents for the present report. A spread sheet was created for these 2,710 samples that includes concentrations for 22 elements (Cu, Pb, Zn, Ag, Au, Hg, As, Sb, Ba, Bi, Mo, Fe, Mg, Ca, Ti, Co, Cr, Ni, V, Sr, Sn, and W). Those elemental analyses reported as "less than lower determination limit" or "not detected" in the original data base were substituted with values at 50 percent of the lower limit of determination (see also, Sanford and others (1993) for a discussion of the suitability of performing such substitutions); analyses reported as "greater than upper limit of determination" were substituted with values of the upper limit of determination. In addition, multiple samples were collected at many of the sample sites. For example, several samples representative of various types of iron oxide-impregnated fault gouge and (or) fault breccia, as well as the least altered-appearing rock of the host formation or igneous body, may have been collected at a single site. The samples excluded for the present study from the modified database primarily

were those (1) that we did not have an adequate latitude and longitude at the time of conversion of the original database, which was based on mining company coordinates, to the modified one based on latitudes and longitudes, or (2) that were from a site judged to be adequately represented geochemically by another sample from that same site. One surprising consequence is that the 217 samples excluded from the database are rather uniformly distributed across the entire area—as a result, the exclusion of these samples should not contribute an inherent systematic sampling bias that would impact any judgments we make from evaluations of the modified database.

Gridding and filtering procedures

The scattered data of the modified database were interpolated to a square grid (using grid intervals 50 m, 100 m, and 500 m) by means of a routine based on the principal of minimum curvature (Briggs, 1974). As a cautionary note, it must be emphasized that the gridding procedures employed are relatively sensitive to the density and uniformity of sampling sites in small domains. This does not result in total disappearance of anomalies or in the appearance of spurious anomalies, but the presence of a large number of samples with relatively low concentrations in a domain surrounding a small number of samples with high concentrations of that element can result in severe damping of the level of the anomaly. An example of this phenomenon is discussed more fully below. In addition, the gridded map data were spatially filtered in an effort to emphasize the broad (long-wavelength) characteristics of the geochemical anomalies by suppressing the narrow (short wavelength) components. With the specific filter used in this study, the shorter the wavelength, the greater the suppression. The magnitude of the relative suppression between any two wavelengths is controlled in this filter by a free parameter z, which has dimensions of length. Short-wavelength characteristics of the data are more strongly attenuated by filters with large values of z. Thus, filters with large values of z are more effective in emphasizing long-wavelength characteristics of anomalies. The type of filter used in this study, when applied to gravity or magnetic data, is known as the "upward continuation" filter (Blakely, 1994), because for a given value of z, the filtered data appear as if they had been measured on a surface that is distance z above the original data surface. The computer-based filtering used in our study is quite analogous to the visual filter applied to down-hole geochemical data by Chaffee (1982).

Tests of the gridding procedure

As noted above, tests of the data at various grid sizes and filtering levels revealed that calculations of the average value for a particular cell of the grid can be influenced highly by the numbers of samples and the values of that element's concentrations in samples in the area of the cell. For example, the highest mercury content calculated without filtering in 50–m grid cells at the Sonderman Prospects is 600 to 700 parts per billion (ppb) Hg—a concentration, which when

considered together with its areal extent, is not that particularly noteworthy (fig. 3). Surface projection of the orebodies "undiscovered" at the time of the sampling could not be shown on this figure and the succeeding ones (figs. 4, 5) because of an incompatibility between computer software programs. They are shown on all succeeding figures. Note, however, that there are a number of mercury anomalies along Galena Ridge (an informally named ridge southwest of the townsite of Galena) that are defined by cells containing greater than 1,400 ppb Hg. On the one hand, the mercury anomaly at the Sonderman prospects has been damped significantly by the large number of samples in the surrounding area that contain 20 to 200 ppb Hg. This occurs even though as many as10 samples from the Sonderman prospects contain 10,000 ppb Hg in the modified database (some samples actually are reported as containing more than 10,000 ppb Hg in the original database, which is the upper limit of determination). On the other hand, the strength of the anomalies along Galena Ridge partly results from sparse numbers of unmineralized samples which are well away from the actual trace of the ridgeline, and, thus, are not included in determinations of the elemental concentrations of cells centered on the ridge. Most samples along the ridge have 210 ppb to as much as 5,000 ppb Hg (fig. 2), and there are only a small number of other samples that fall within 50–m wide cells because of the absence of exposures. At a 50–m cell spacing, there are no unmineralized samples in the immediate area to depress the strength of the anomalies along the ridge. Therefore, the gridding procedure probably is best suitable for a uniform density of samples in an area. Nonetheless, gridding procedures have been used fairly routinely in some regional geochemical exploration programs (Voynovski and Kotlyar, 1988).

Preliminary cell size and filter parameter tests

Some preliminary tests of the geologic applicability of the proposed filtering procedures involved gridding the geochemical data at Copper Canyon to 50–m-wide cells, and applying a moderate wave length filter parameter of 100 m—this is exemplified by the distribution for mercury (fig. 4). Filtering of data results in a reduction of the geochemical "noise" due to wide fluctuations of elemental concentrations among nearby samples, emphasizes the broad or more wide-ranging characteristics of an anomaly, and provides a visual anomaly contrast that is difficult to synthesize from the spot maps of the geochemical data (compare figs. 1*D*, 2–4). After many attempts using various combinations of cell sizes and filter parameter z, it appeared that a reasonable combination for the dataset at Copper Canyon involved a cell size of 100 m and a z value of 100 m (fig. 4). The resulting contours with a 50–m cell size and a z value of 100 m show "more geologic appearing" contours (fig. 5).

Data evaluation using 100–m cells and z factors of 100 m

Machine-contoured plots for Mo, Cu, Au, Ag, Sn, As, Hg, Pb, Zn, Bi, and Sb were prepared from the database using 100–m-wide cells and a z factor of 100 m (fig. 6*A–K*). Also

shown on the figures are the surface projection of the large ore bodies that were unexposed in the area at the time of geochemical sampling, as well as the East ore body (stippled pattern, fig. 6), which was in its early stages of stripping and mining. Distribution of high concentrations of molybdenum are controlled largely by the extent of surface exposures of the altered granodiorite of Copper Canyon. Many of the metal deposits and occurrences, both large and small, are outside most of the contoured elevated concentrations of molybdenum. High concentrations of copper are also controlled largely by area of outcrop of the altered granodiorite of Copper Canyon, which has been enhanced near the surface by supergene, downslope migration of copper from the once topographically high East orebody as discussed above. The distribution of the highest concentrations of copper (>500 ppm Cu, fig. 6*B*) is somewhat broader than that shown in figure 1*B* because the highest contour shown in the latter is >700 ppm Cu. In addition, there is a an elevated abondance of copper (>500 ppm Cu. fig. 6*B*) in the general area of the Wilson-Independence Mine and the small exposures of the altered granodiorite of Copper Canyon approximately 500 m farther to the north. The level of abundance of copper in these small exposures probably results from in-place secondary copper derived from dispersed hypogene chalcopyrite. The machine-contoured plots for Au, Ag, Sn, As, Hg, and Pb (fig. 6*C–H*) all show various degrees of development of a semi-annular ring, annular, or hook-shaped pattern of elevated abundances around the four major ore bodies (Lower Fortitude, Upper Fortitude, Phoenix, and West ore body) north of the main exposures of the altered granodiorite of Copper Canyon. These patterns of geochemical zonation are generally consistent with those proposed for porphyry systems (Jones, 1992: Albino, 1993). All of these deposits at Copper Canyon are base- and precious-metal skarn orebodies with the exception of the Upper Fortitude orebody which is predominantly a fracture-controlled replacement orebody controlled largely by the Virgin fault. The most striking of these plots with respect to zonation relative to the orebodies is perhaps that for mercury (fig.6*G*). Partly on the basis of these plots, we suggest that all of these metals were introduced into various host rocks and faults as part of a single protracted mineralizing event, in places and at times associated with development of skarn and elsewhere with potassic alteration assemblages, as well as with all the retrograde mineral assemblages common to a porphyry copper environment. Although mercury is not a metal commonly considered to be associated with orebodies in this type of geologic environment (Bailey and others, 1973; Chaffee, 1982), it appears incontrovertible from these data at Copper Canyon that mercury forms a significant halo or fringing anomaly to the largest orebodies north of the altered granodiorite of Copper Canyon. Nonetheless, this relation of mercury at Copper Canyon is somewhat consistent with the classical schematic zonation of mercury proposed by Emmons (1927). At Copper Canyon, however, the bulk of the mercury in pre-mining exposures appears to have been present near the innermost limit of the lead-zinc zone. The continuation of high concentrations of mercury into the East orebody as shown on the plot (fig. 6*G*) is verified by contents of commonly >10,000 ppb Hg along mineralized faults, many containing abundant arsenopyrite, in the East orebody (Theodore and

Blake, 1975). We currently have underway studies using a scanning electron microscope to establish the mineral-occurrence site(s) of mercury in mineralized rocks north of the Lower Fortitude orebody.

In addition, there appears to be a marked assymetry in the distribution and concentrations of mercury north of the altered granodiorite of Copper Canyon versus that south of the altered granodiorite of Copper Canyon (fig. 6*G*). The southern part of the Copper Canyon area appears to be significantly depleted with respect to mercury—this is especially true for the southwestern part of the area near the Wilson-Independence Mine. However, contents of mercury generally appear to be increasing near the southernmost parts of the Copper Canyon area near the southern part of the Midas orebody as well as south of the Tomboy Mine. There are several explanations, and a combination of circumstances, that may have contributed to this asymmetry. The entire mineralized system and its host rocks may be tilted downwards to the north because of the presence of widely exposed bodies of the Antler sequence south of the altered granodiorite of Copper Canyon and their absence north of the altered granodiorite of Copper Canyon. However, the possibility of tilting about an east-west axis is weakened by the absence of evidence for this in the geology, and by our judgment that the highest temperature parts of the entire system are north of the altered granodiorite of Copper Canyon and not south of it as well they should be if the complex were tilted to the north. It is also possible that we do not have the entire north-south breadth of the mineralized system exposed at Copper Canyon, and that some parts of it remain covered by Quaternary gravels and alluvium farther to the south. Alternatively, most of the inferred southern parts of the Copper Canyon system may have been eroded away, as well as their being some elevation effects that contribute to metal distribution. There are approximately 5,300–ft elevations at the mouth of Copper Canyon, and approximately 6,400–ft pre-mining elevations at the general area of the saddle just to the north of the Fortitude deposit (Theodore and Blake, 1975).

The presence of low, yet anomalous, concentrations of tin in the Copper Canyon area, some of which are coincident with anomalies of Au, Ag, As, Hg, Pb, and Zn (compare figs. 6*E* and 6*C*, *D*, *F–I*), appears to confirm similar associations found for tin in the general area of the Little Giant Mine in the north-central part of the Battle Mountain Mining District (Theodore and others, 1992). At the Little Giant Mine, concentrations are as much as 100 ppm Sn along the silver-zinc-arsenic-gold veins and fault breccias there. This mineralization apparently is associated genetically with a small, 38– to 40–Ma rhyolite intrusion approximately 0.7 km south of the Late Cretaceous Buckingham stockwork molybdenum system.

Data evaluation using 100–m cells and *z* factors of 500 m

Machine-contoured plots for Mo, Cu, Au, Ag, Sn, As, Hg, Pb, Zn, Bi, and Sb also were prepared from the database using 100–m-wide cells and a *z* factor of 500 m (fig. 7*A–K*).

Although highly generalized, the plots illustrate broad elemental distributions previously determined in the Copper Canyon area (Roberts and Arnold, 1965; Theodore and Blake, 1975; Wotruba and others, 1986; Myers, 1994), and they provide further insight into the evolution of the magmatic-hydrothermal system. The plots also may be viewed as yielding overall lithogeochemical relations among metals that constitute ore and those indicator metals distal to ore (Beus and Grigorian, 1977). However, we must emphasize, as we did previously above, that the domains underlain by the respective contour intervals for various metals must not be construed as implying that all rocks in these domains contain abundances of metals equal to that bracketed by the contour intervals. Generally, there is a strong bimodality of elemental concentrations throughout the entire area that is marked by those rocks which are, on the one hand, mineralized strongly along faults, and, on the other hand, those less so in rocks between faults. Although, these plots are extremely generalized, they portray well many aspects of lithogeochemistry at Copper Canyon. Their usage may have applications in small-scale surveys where general centers of mineralization are being sought in a mining district or inter-mining district relations are being determined, as well as in regional stream-sediment geochemical surveys and geoenvironmental studies.

Plots of elemental distributions of molybdenun and copper using 100–m cells for gridding and a *z* factor of 500 m generally duplicate the broad aspects of the previous plots for these elements at a z factor of 100 m (fig. 7*A*, *B*). Molybdenum shows a pair of assymetric bipolar anomalies directly over the two areas of outcrop of the altered granodiorite of Copper Canyon—the stronger of the anomalies (>20 ppm Mo) coincides with the main area of outcrop of granodiorite of Copper Canyon west-southwest of the East orebody. The plot for copper (fig. 7*B*) is quite similar to the plot for molybdenum, and shows a large anomaly (>1,000 ppm Cu) centered south of the East orebody. However, it must be recalled that the two major ore bodies at Copper Canyon mined primarily for their copper content, the East and West ore bodies, are not coincident with the major molybdenum anomalies.

The contoured plot for gold (fig. 7*C*) displays its strongest anomaly (>300 ppb Au) in the general area of the Wilson-Independence Mine, west of Copper canyon, which is an underground mine developed along a north-south veined fault system. This anomaly coincides with a similar-sized one for arsenic (>700 ppm As, fig. 7*F*). In addition, there are two other major anomalies for gold detected using a 100–m grid and z factor of 500 m. One of these is centered just east of the Phoenix deposit and the other near the northeast corner of the area. All gold anomalies in the area appear to define a broadly northeast-elongate zone that contains elevated abundances for gold and that traverses the entire area—also roughly coincident with the overall shape of the distribution pattern for bismuth (fig. 7*J*). It is interesting to note that there appears to be a northeast trend to the highest concentrations of gold in parts of the Fortitude deposit (Doebrich and others, 1995). The

strongest anomaly of bismuth (>20 ppm Bi) also is coincident with the anomalies for gold and arsenic at the Wilson-Independence Mine, and the strength of this bismuth anomaly relative to the others may also be a reflection of a "geochemically deeper" part of the system on the south—this may be due to deeper erosion on the south than on the north. The gold anomalies detected include copper, bismuth, molybdenum, and arsenic at Copper Canyon. A positive association between free gold, electrum, arsenopyrite, and native bismuth has been well established in the Fortitude gold skarn deposit (Myers, 1994). In porphyry copper systems elsewhere, Beus and Grigorian (1977) note that arsenic is generally present in the distal parts of the hypogene systems.

The contoured plots for silver, tin, lead, and zinc (fig. 7*D*,*E*, *H*, *I*) all show a north-south grain to their distributions, as well as a strong spatial coincidence among many components common to each of the individual plots. These elements are concentrated, possibly with the exception of tin, generally outside the pyritic halo that surrounds the altered granodiorite of Copper Canyon (fig. 1*A*), and they are a geochemical association common to the polymetallic veins that surround the center of the system (Roberts and Arnold, 1965). The patterns for lead and zinc, in particular, suggest a continuation of these anomalies north of the Copper Canyon area, which is in agreement with the presence of the most productive lead-zinc-silver polymetallic veins in the mining district at the White and Shiloh Mine approximately 0.3 km farther to the north (Roberts and Arnold, 1965).

The contoured plot for antimony shows its highest concentrations (>125 ppm Sb, fig. 7*K*) to include two of the polymetallic vein occurrences at the Buena Vista Mine north of the pyrite halo that surrounds the porphyry system at Copper Canyon. Most antimony appears to be associated with a single broad anomaly that is elongated along a northeast trend, and that generally lies beyond and distal to the similarly elongate anomaly for bismuth. There is a minor geochemical anomaly for bismuth at the Wilson-Independence Mine (25 to 50 ppm Sb, fig. 7*K*), which, when compared to the stronger aforementioned anomaly near the Buena Vista Mine, might also be a reflection of deeper erosion of the geochemical system on the south. In addition, the bulk of the area showing presence of detectable antimony on this plot is underlain by rocks of the Havallah sequence, which comprises the structurally highest package of Paleozoic rocks in the area.

The contoured plot for mercury at a 100–m grid and a *z* factor equal to 500 m coalesces into a broad geochemical anomaly that is centered at approximately the polymetallic vein occurrence at the Nevada Mine, just to the north of the Fortitude deposit, and that is defined by a domain apparently underlain by elevated concentrations of mercury (>200 ppb Hg, fig. 7*G*). This domain also includes the polymetallic veins at the Buena Vista Mine. In addition, there is a suggestion that elevated mercury abundances continue to the north beyond the Copper Canyon area, and that, possibly, they may also continue to the northeast—extending thereby through the northeast corner of the area. In the southern part of the Copper Canyon area, the contoured plot for

mercury also shows a progressive increase in mercury concentrations that appears to extend beyond the southern boundary of the area. This latter anomaly cannot extend much farther to the south, however, because there is not much more bedrock exposed in this part of the mining district. Nonetheless, the two mercury anomalies appear to define a "dumbbell"-shaped pattern that has its northern part much more strongly developed than the southern one. This relation for mercury also is consistent with a deeper erosion of the geochemical system on the north.

Summary and conclusions

Our re-examination, by modern contouring procedures, of geochemical data from rocks surrounding the largely skarn-related porphyry copper deposits at Copper Canyon have revealed a number of associations and relations that previously were not that apparent. The most striking, perhaps, is the presence of a well-developed halo of elevated mercury abundances marginally distal to some of the larger gold-skarn ore deposits formed on the north flank of the altered granodiorite of Copper Canyon. This halo was defined by a 100–m grid and a *z* factor equal to 100 m. Finally, examination of the generalized distribution patterns for mercury, bismuth, and antimony at a 100–m grid and a z factor equal to 500 m suggests that, although there may have been some downward tilting of the mineralized system about an east-west axis, the most likely explanation is that the southern parts of the system are more deeply eroded than the parts north of the altered granodiorite of Copper Canyon. These geochemical studies of bedrock exposures established some metal zonations which are currently being linked to the third dimension—including three-dimensional arrays of metal distributions around the Lower Fortitude deposit.

References cited

Albino, G.V., 1993, Application of metal zoning to gold exploration in porphyry copper systems by B.K. Jones: comments: Journal of Geochemical Exploration, v. 48, no 3, p. 359–366.

Bailey, E.H., Clark, A.L., and Smith, R.M., 1973, Mercury, *in* Brobst, D.A., and Pratt, W.P., eds., United States mineral resources: U.S. Geological Survey Professional Paper 820, p. 401–414.

Beus, A.A., and Grigorian, S.V., 1977, Geochemical exploration methods for mineral deposits: Wilmette, Illinois, Applied Publishing Ltd., 287 p.

Blakely, R.J., Potential theory in gravity and magnetic applications: New York, Cambridge University Press, 441 p.

Briggs, I.C., 1974, Machine contouring using minimum curvature: Geophysics, v. 39, p. 39–48.

Chaffee, M.A., 1982, A geochemical study of the Kalamazoo porphyry copper deposit, *in* Titley, S.R., ed., Advances in geology of the porphyry copper deposits: Tucson, Arizona, The University of Arizona Press, p. 211–225.

Doebrich, J.L., 1995, Geology and mineral deposits of the Antler Peak 7.5–minute quadrangle, Lander County, Nevada: Nevada Bureau of Mines and Geology Bulletin 109, 44 p.

Doebrich, J.L., Wotruba, P.R., Theodore, T.G., McGibbon, D.H., and Felder, R.P., 1995, Field guide for geology and ore deposits of the Battle Mountain Mining District, Humboldt and Lander Counties, Nevada: Reno, Nevada, Geological Society of Nevada and U.S. Geological Survey, Great Basin Symposium III, Geology and ore deposits of the American Cordillera, 92 p.

Emmons, W.H., 1927, Relations of metalliferous lode systems to igneous intrusives: Transactions of the American Institute of Mining and Metallurigical Engineers, v. 74, p. 29–70.

Grimes, D.J., and Marranzino, A.P., 1968, Direct-current arc and alternating-current spark emission spectrographic field methods for the semiquantative analysis of geologic materials: U.S. Geological Survey Circular 591, 6 p.

Haffty, Joseph, Riley, L.B., and Goss, W.D., 1977, A manual on fire assaying and determination of the noble metals in geological materials: U.S. Geological Survey Bulletin 1443, 58 p.

Hammarstrom, J.M., Elliott, J.E., Kotlyar, B.B., Theodore, T.G., Nash, J.T., John, D.A., Hoover, D.B., and Knepper, D.H., Jr., 1995, Sn and (or) W skarn and replacement deposits, *in* Dubray, E.A., ed., Preliminary compilation of geoenvironmental mineral deposit models: U.S. Geological Survey Open-File Report (in press).

Hammarstrom, J.M., Elliott, J.E., Theodore, T.G., Kotlyar, B.B., Doebrich, J.L., Elliott, J.E., Nash, J.T., and John, D.A., 1995, Fe skarn deposits, *in* Dubray, E.A., ed., Preliminary compilation of geoenvironmental mineral deposit models: U.S. Geological Survey Open-File Report (in press).

Hammarstrom, J.M., Kotlyar, B.B., Theodore, T.G., Elliott, J.E., John, D.A., Doebrich, J.L., and Nash, J.T., 1995a, Cu, Au, and Pb-Zn skarn deposits, *in* Dubray, E.A., ed., Preliminary compilation of geoenvironmental mineral deposit models: U.S. Geological Survey Open-File Report (in press).

Jones, B.K., 1992, Application of metal zoning to gold exploration in porphyry copper systems: Journal of Geochemical Exploration, v. 43, no. 2, p. 127–155.

Myers, G.L., 1994, Geology of the Copper Canyon-Fortitude skarn system, Battle Mountain, Nevada: Pullman, Washington, Washington State University, Ph.D. dissertation, 338 p.

Roberts, R.J., 1964, Stratigraphy and structure of the Antler Peak quadrangle, Humboldt and Lander Counties, Nevada: U.S. Geological Survey Professional Paper 459–*A*, 93 p.

Roberts, R.J., and Arnold, D.C., 1965, Ore deposits of the Antler Peak quadrangle, Humboldt and Lander Counties, Nevada: U.S. Geological Survey Professional Paper 459–*B*, 94 p.

Roberts, R.J., Hotz, P.E., Gilluly, James, and Ferguson, H.G., 1958, Paleozoic rocks in north-central Nevada: American Association of Petroleum Geologists Bulletin, v. 42, no. 12, p. 2,813–2,857.

Sanford, R.F., Pierson, C.T., and Crovelli, R.A., 1993, An objective replacement method for censored geochemical data: Mathematical Geology, v. 25, no. 1, p. 59–80.

Silberling, N.J., and Roberts, R.J., 1962, Pre-Tertiary stratigraphy and structure of northwestern Nevada: Geological Society of America Special Paper 72, 58 p.

Theodore, T. G., 1969, Surface distribution of selected elements around the Copper Canyon copper-gold-silver open pit mine, Lander County, Nevada: U.S. Geological Survey Open-File Report 69–278, 1 p. plus 22 sheets.

———1970, Rock analyses around the Copper Canyon open pit mine, Lander County, Nevada: U.S. Geological Survey Open-File Report 70–325, 2 p., plus 236 p tabular material, 4 plates.

Theodore, T.G., and Blake, D.W., 1975, Geology and geochemistry of the Copper Canyon porphyry copper deposit and surrounding area, Lander County, Nevada: U.S. Geological Survey Professional Paper 798–*B*, p. *B*1–*B*86.

———1978, Geology and geochemistry of the West ore body and associated skarns, Copper Canyon porphyry copper deposits, Lander County, Nevada, *with a section on* Electron microprobe analyses of andradite and diopside by N.G. Banks: U.S. Geological Survey Professional Paper 798–*C*, p. *C*1–*C*85.

Theodore, T.G., Blake, D.W., Loucks, T.A., and Johnson, C.A., 1992, Geology of the Buckingham stockwork molybdenum deposit and surrounding area, Lander County, Nevada, *with a section on* Potassium-argon and $^{40}Ar/^{39}Ar$ geochronology of selected plutons in the Buckingham area, by E.H. McKee, *and a section on* Economic geology, by T.A. Loucks and C.A. Johnson, *and a section on* Supergene copper deposits at Copper Basin by D.W. Blake, *and a section on* Mineral chemistry of Late Cretaceous and Tertiary skarns, by J.M. Hammarstrom: U.S. Geological Survey Professional Paper 798–*D*, 307 p.

Theodore, T.G., Howe, S.S., Blake, D.W., and Wotruba, P.R., 1986, Geochemical and fluid zonation in the skarn environment at the Tomboy-Minnie gold deposits, Lander County, Nevada: Journal of Geochemical Exploration, v. 25, p. 99–128.

Theodore, T.G., and Nash, J.T., 1973, Geochemical and fluid zonation at Copper Canyon, Lander County, Nevada: Economic Geology, v. 68, no. 4, p. 565–570.

Theodore, T.G., Silberman, M.L., and Blake, D.W., 1973, Geochemistry and K–Ar ages of plutonic rocks in the Battle Mountain mining district, Lander County, Nevada: U.S. Geological Survey Professional Paper 798–*A*, 24 p.

Voynovski, A.S., and Kotlyar, B.B., 1988, The potential of molybdenum ore deposits in the Ustinov massif: Geologicheskiy Journal, no. 6, p.59–65. [in Russian]

Wilson, S.A., Kane, J.S., Crock, J.G., and Hatfield, D.B., 1987, Chemical methods of separation for optical emission, atomic absorption spectrometry, and colorimetry, *in* Baedecker, P.A., ed., Methods for geochemical analysis: U.S. Geological Survey Bulletin 1770, p. *D*1–*D*14.

Wotruba, P.R., Benson, R.G., and Schmidt, K.W., 1986, Battle Mountain describes the geology of its Fortitude gold-silver deposit at Copper Canyon: Mining Engineering, July 1986, v. 38, no. 7, p. 495–499.

FIGURE CAPTIONS

Figure 1.—Maps showing geology (*A*), and hand-contoured distribution of copper (*B*), lead (*C*), mercury (*D*), arsenic (*E*), and cadmium (*F*) in 2,927 rock samples at Copper Canyon, Battle Mountain Mining District, Nev. Geochemical data from Theodore (1969, 1970). geology modified from Theodore and Blake (1975), and surface projection of ore deposits from Doebrich and others (1995).

Figure 2.—Spot map showing distribution of mercury in 2,927 rock samples at Copper Canyon, Nev. Modified from Theodore (1969).

Figure 3—Plot of mercury concentrations, in parts per billion, using a 50–m grid and *z* factor equal to zero for 2,710 rock samples extracted from the 2,927–sample database of Theodore (1970) at Copper Canyon, Nev.

Figure 4—Plot of mercury concentrations, in parts per billion, using a 100–m grid and *z* factor equal to 100 m for 2,710 rock samples extracted from the 2,927–sample database of Theodore (1970) at Copper Canyon, Nev.

Figure 5—Plot of mercury concentrations, in parts per billion, using a 50–m grid and *z* factor equal to 100 m for 2,710 rock samples extracted from the 2,927–sample database of Theodore (1970) at Copper Canyon, Nev.

Figure 6—Plot of machine-contoured concentrations of molybdenum (*A*), copper (*B*), gold (*C*), silver (*D*), tin (*E*), arsenic (*F*), mercury (*G*), lead (*H*), zinc (*I*), bismuth (*J*), and antimony (*K*) using a 100–m grid and *z* factor equal to 100 m for 2,710 rock samples extracted from the 2,927–sample database of Theodore (1970) at Copper Canyon, Nev. Stippled area is East ore body, which was only area of substantial ground disturbance at time of sample collection.

Figure 7—Plot of machine-contoured concentrations of molybdenum (*A*), copper (*B*), gold (*C*), silver (*D*), tin (*E*), arsenic (*F*), mercury (*G*), lead (*H*), zinc (*I*), bismuth (*J*), and antimony (*K*) using a 100–m grid and *z* factor equal to 500 m for 2,710 rock samples extracted from the 2,927–sample database of Theodore (1970) at Copper Canyon, Nev. Stippled area is East ore body, which was only area of substantial ground disturbance at time of sample collection.

Figure 1

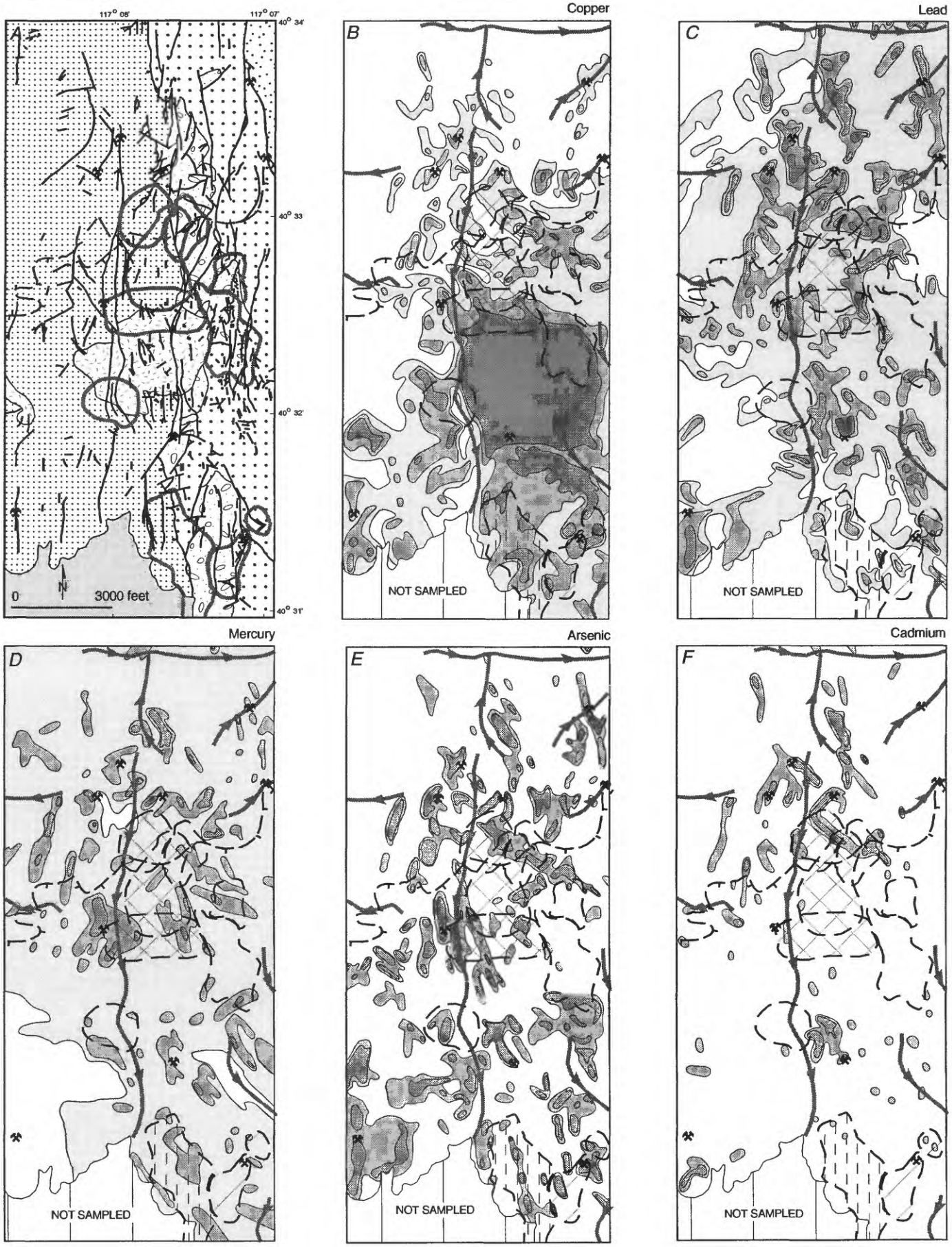
A
117° 08'
117° 07'
40° 34'
40° 33'
40° 32'
40° 31'
0
N
3000 feet
B
Copper
NOT SAMPLED
C
Lead
NOT SAMPLED
D
Mercury
NOT SAMPLED
E
Arsenic
NOT SAMPLED
F
Cadmium
NOT SAMPLED

Figure 1. -- Continued.

EXPLANATION

Younger alluvium and fanglomerate deposits (Quaternary)

Altered granodiorite and quartz diorite (Tertiary)

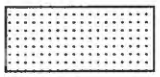

Havallah sequence (Permian, Pennsylvanian, and Missisipian) -- In this area includes only lithotectonic unit 1 of Murchey (1990) (Permian and Pennsylvanian); argillite, shale, and chert

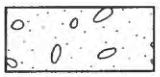

Antler sequence of Roberts (Permian and Pensylvanian) -- Includes conglomerate of Middle Pennsylvanian Battle Formation, limestone of Pennsylvanian and Permian Antler Peak Limestone, and sandstone and conglomerate of Permian Edna Mountain Formation

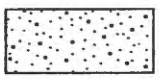

Scott Canyon Formation (Devonian) -- Chert, shale, argillite

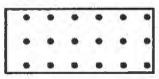

Harmony Formation (Upper Cambrian)-- Mostly feldspathic sandstone

Geological contacts

High angle fault -- bar and ball on side of down-dropped block

Thrust fault -- sawteeth on upper plate

Outer limit of pyritized rocks, hachures on side of pyritized rock

Projection to the surface of outer limit of large disseminated deposits

Small vein deposits and occurrences

Projection to the surface in *B-F* of outer limit of :

Cu, Au, Ag altered porphyry deposits

Cu, Au, Ag skarn deposits, unexposed prior to mining, sulfide

Au, Ag (Pb, Zn, Cu) skarn deposits, exposed prior to mining, sulfide

Au, Ag (Cu, Pb, Zn) skarn deposits, oxidized, exposed prior to mining

Trend of major drainages showing stream-flow direction

Concentrations of select metals in 2,927 rock samples
(in parts per million; N.A., not applicable)

	Copper	Lead	Mercury	Arsenic	Cadmium
	<50	<10	<0.02	<200	<20
	50-150	10-70	0.02-0.2	N.A.	N.A.
	200-700	100-700	0.2-1	200-700	20-50
	>700	>700	>1	>1000	>70

Figure 2.

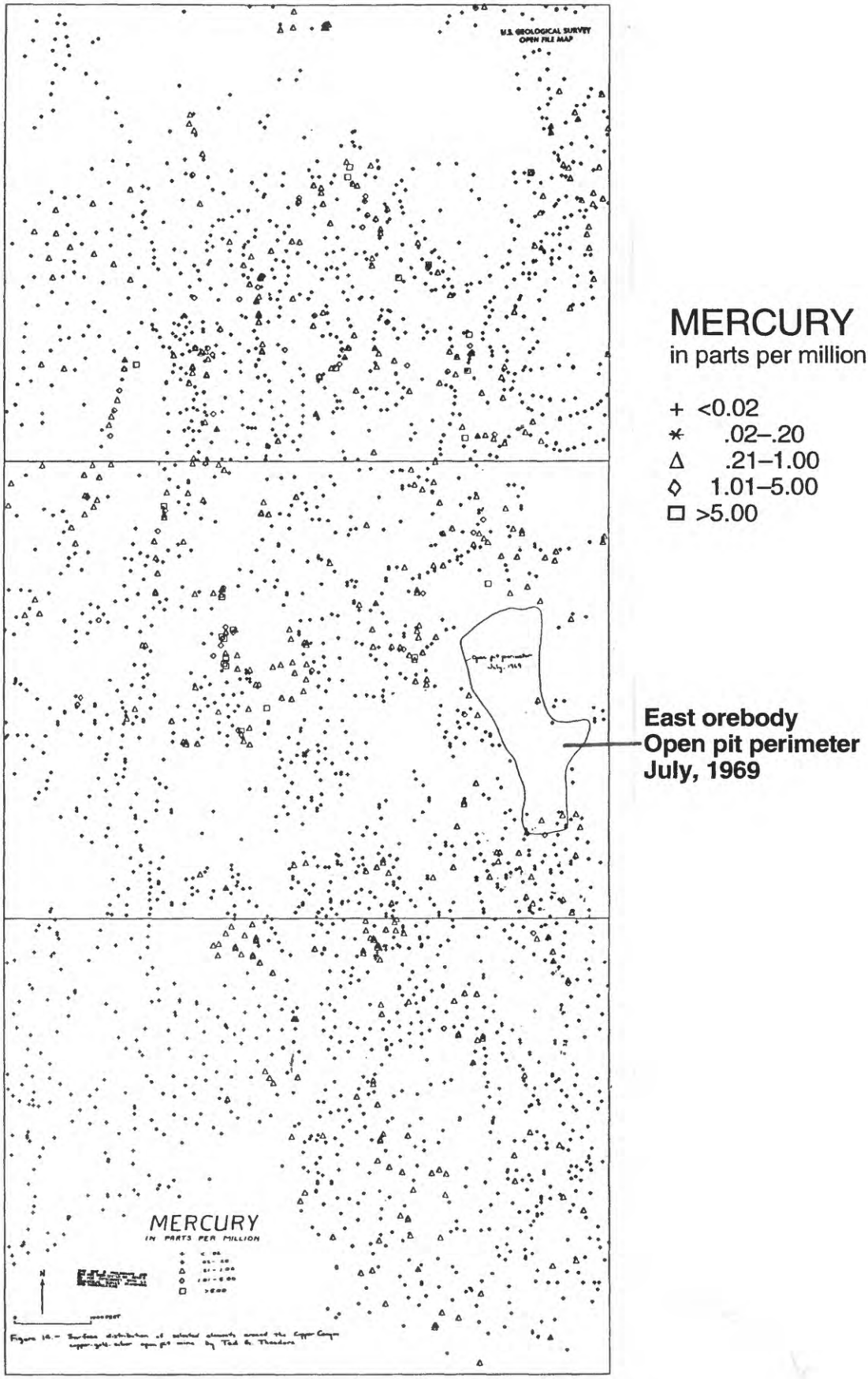
MERCURY
in parts per million
+ <0.02
* .02–.20
Δ .21–1.00
◊ 1.01–5.00
□ >5.00
East orebody
Open pit perimeter
July, 1969
MERCURY
IN PARTS PER MILLION

Figure 3. MERCURY (50 m grid, z=0 m)

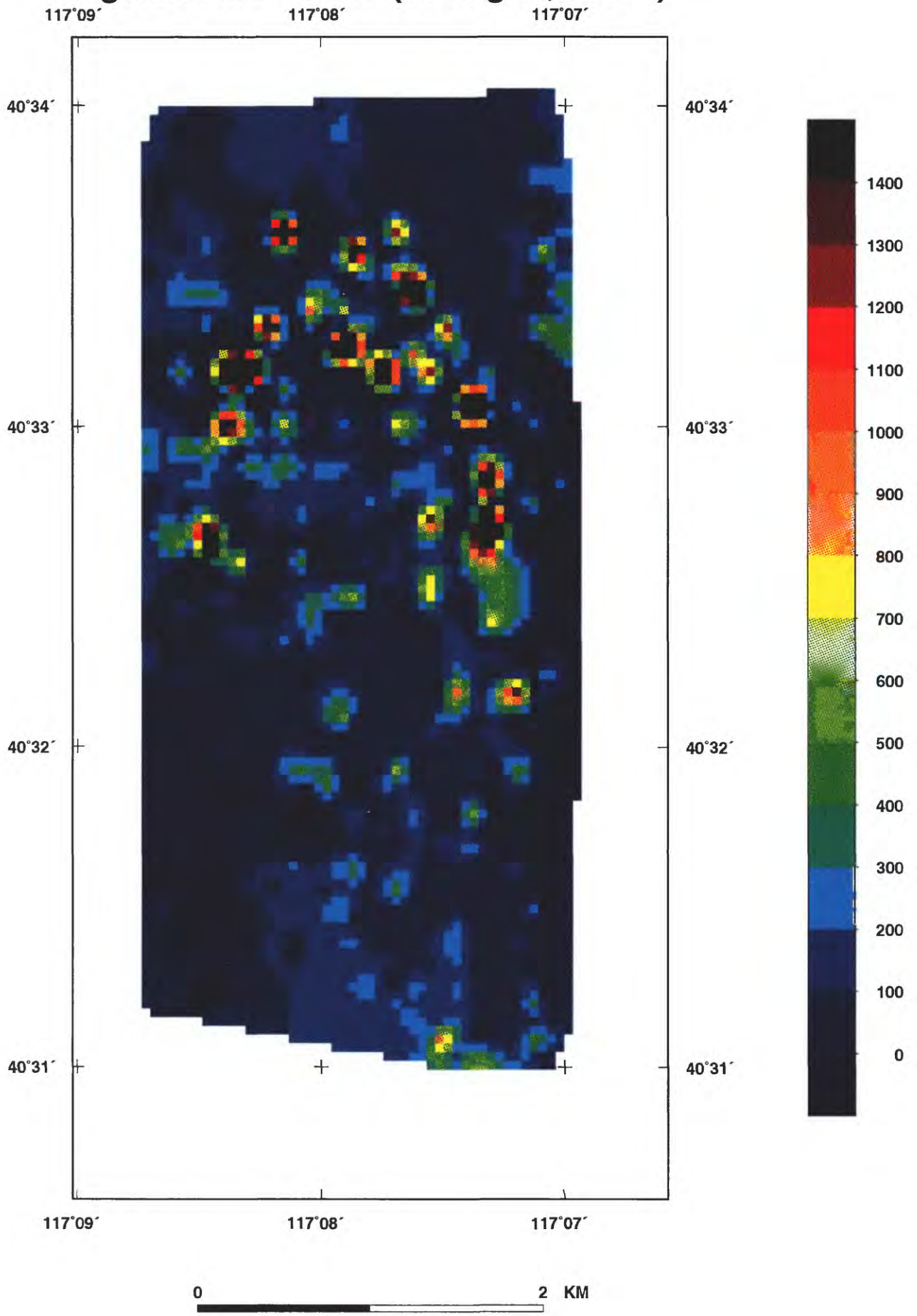

Figure 4. MERCURY (100 m grid, z=100 m)

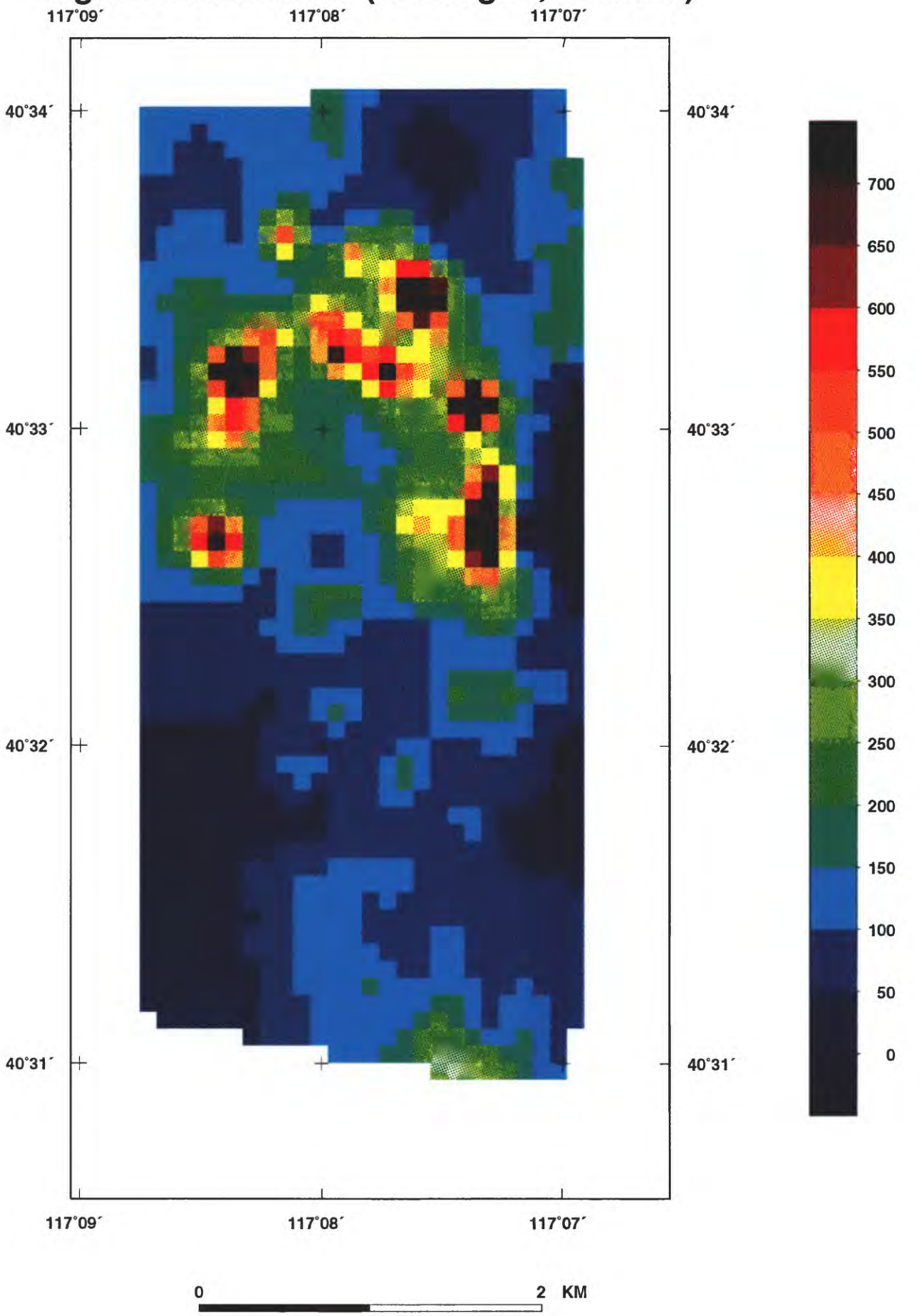

Figure 5. MERCURY (50 m grid, z=100 m)

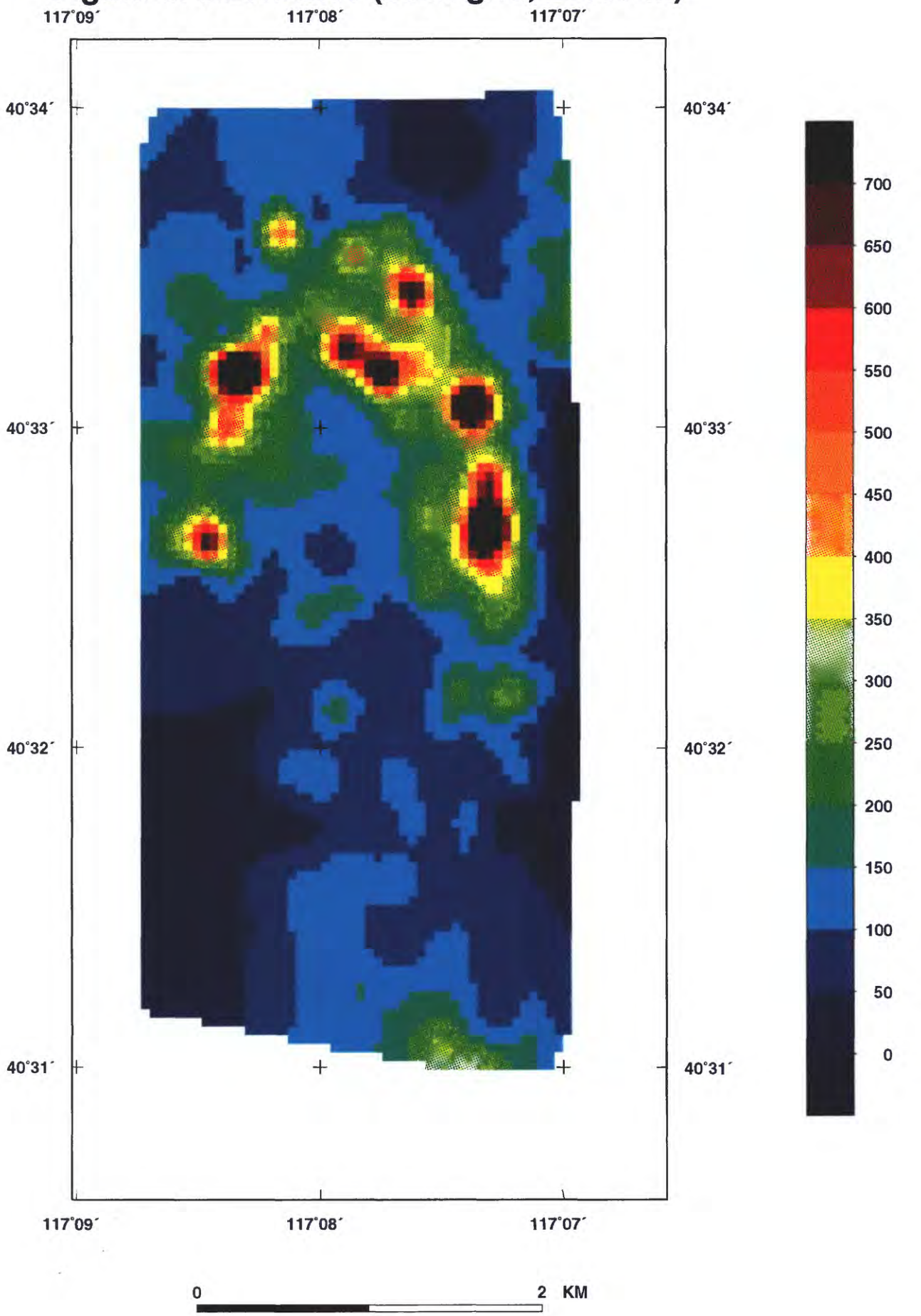

Figure 6.

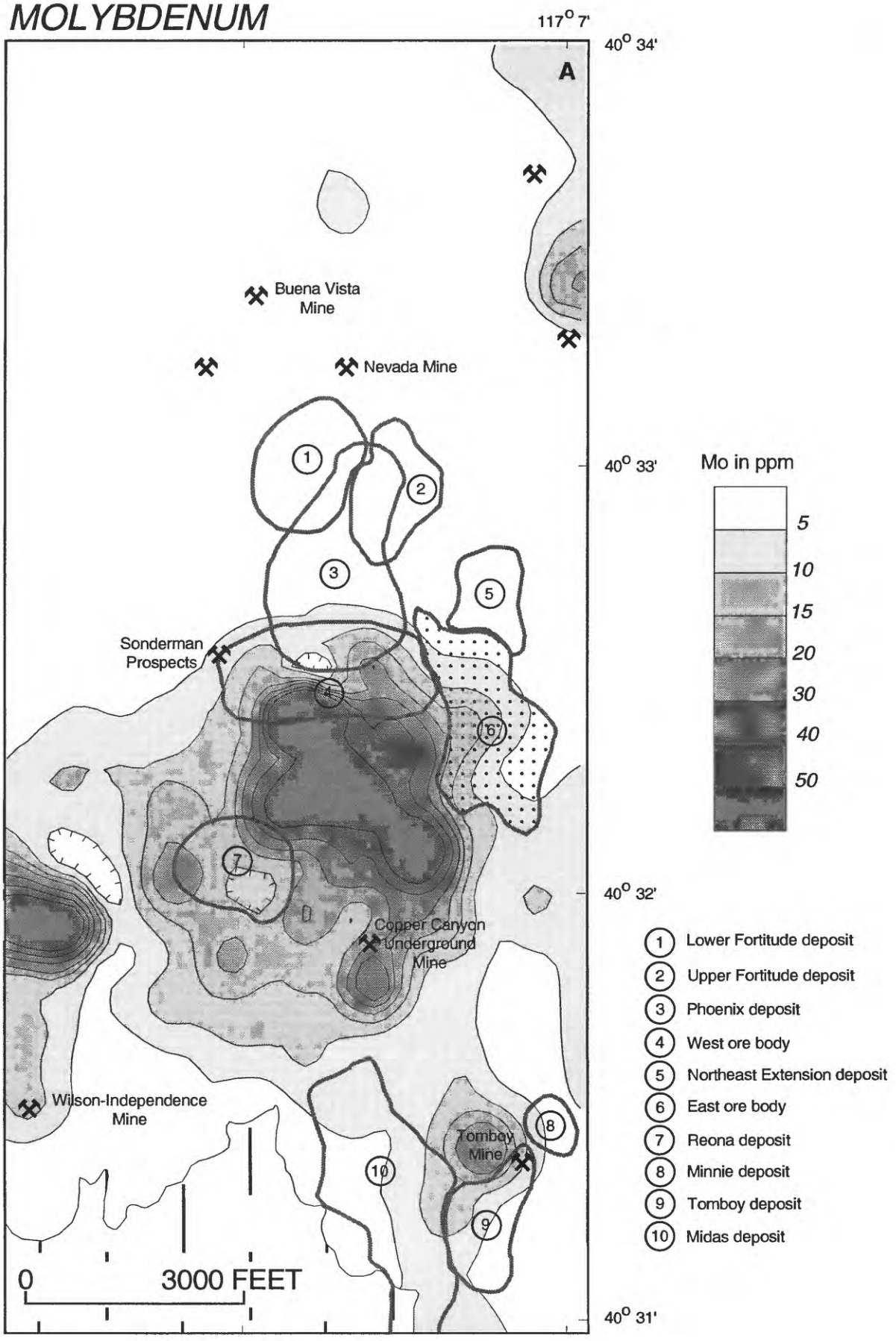
MOLYBDENUM
117° 7'
40° 34'
40° 33'
40° 32'
40° 31'
A
Buena Vista Mine
Nevada Mine
Sonderman Prospects
Copper Canyon Underground Mine
Wilson-Independence Mine
Tomboy Mine
0
3000 FEET
Mo in ppm
5
10
15
20
30
40
50
1 Lower Fortitude deposit
2 Upper Fortitude deposit
3 Phoenix deposit
4 West ore body
5 Northeast Extension deposit
6 East ore body
7 Reona deposit
8 Minnie deposit
9 Tomboy deposit
10 Midas deposit

Figure 6. -- Continued.

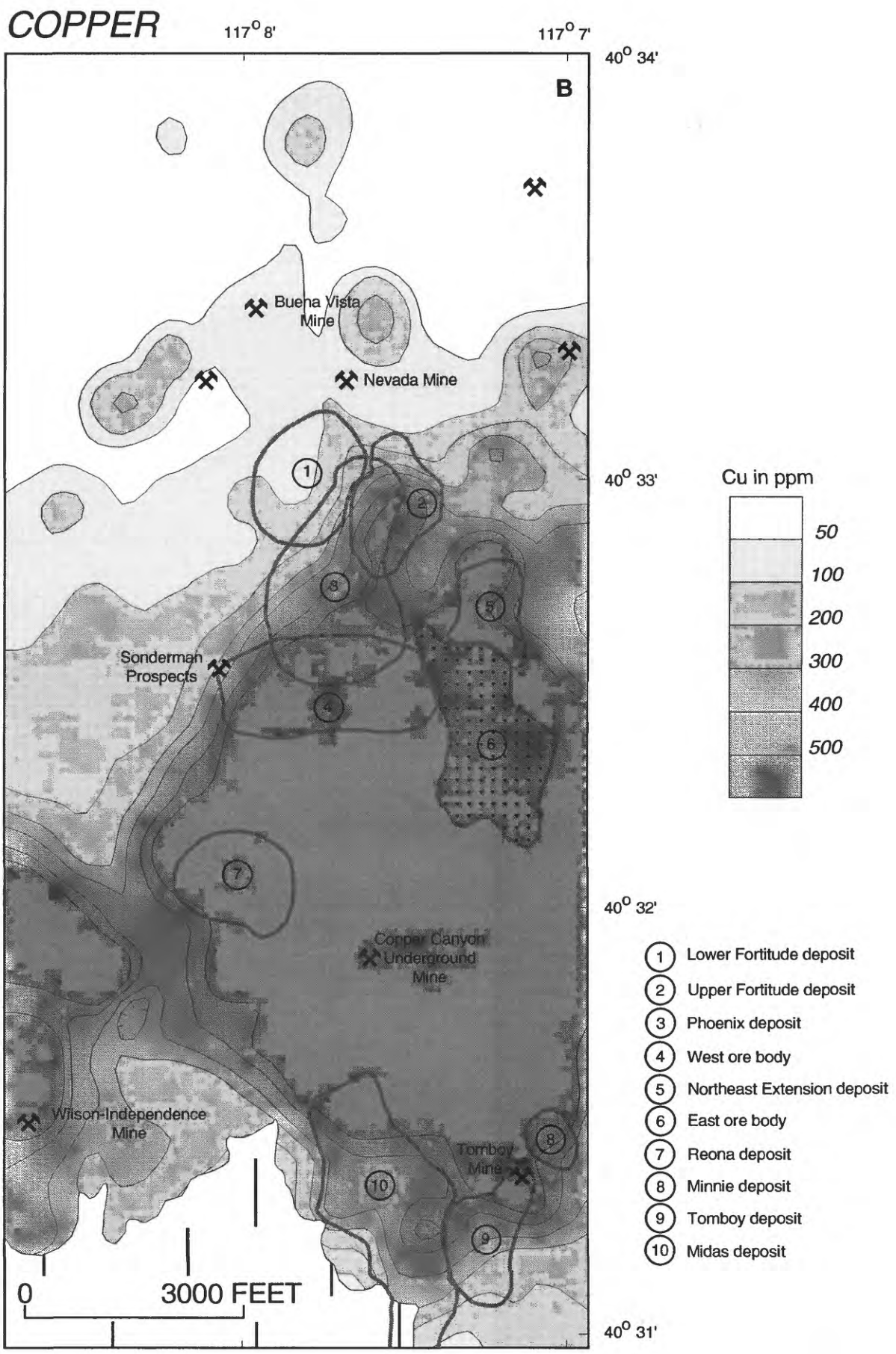

Figure 6. -- Continued.

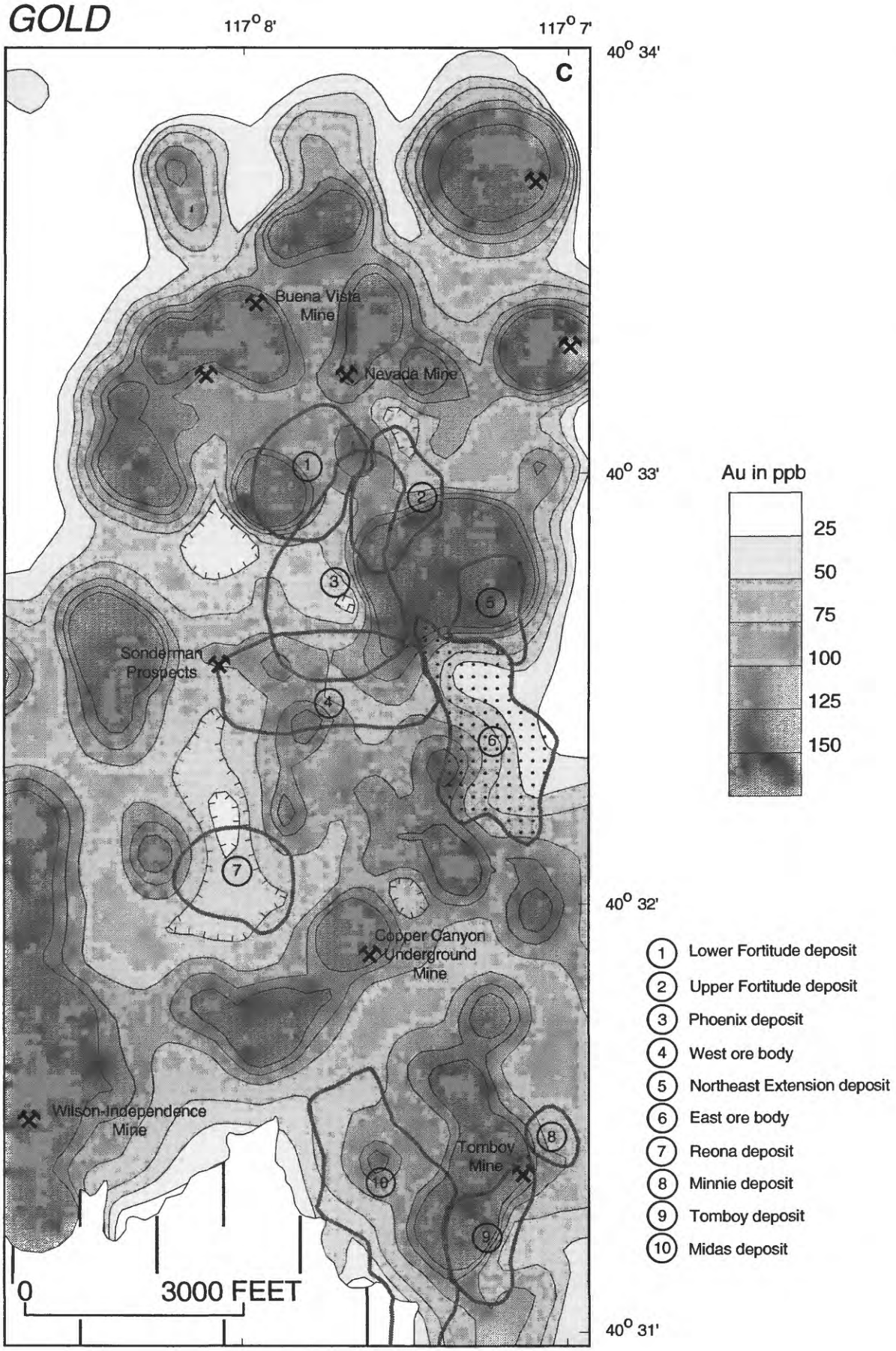

Figure 6. -- Continued.

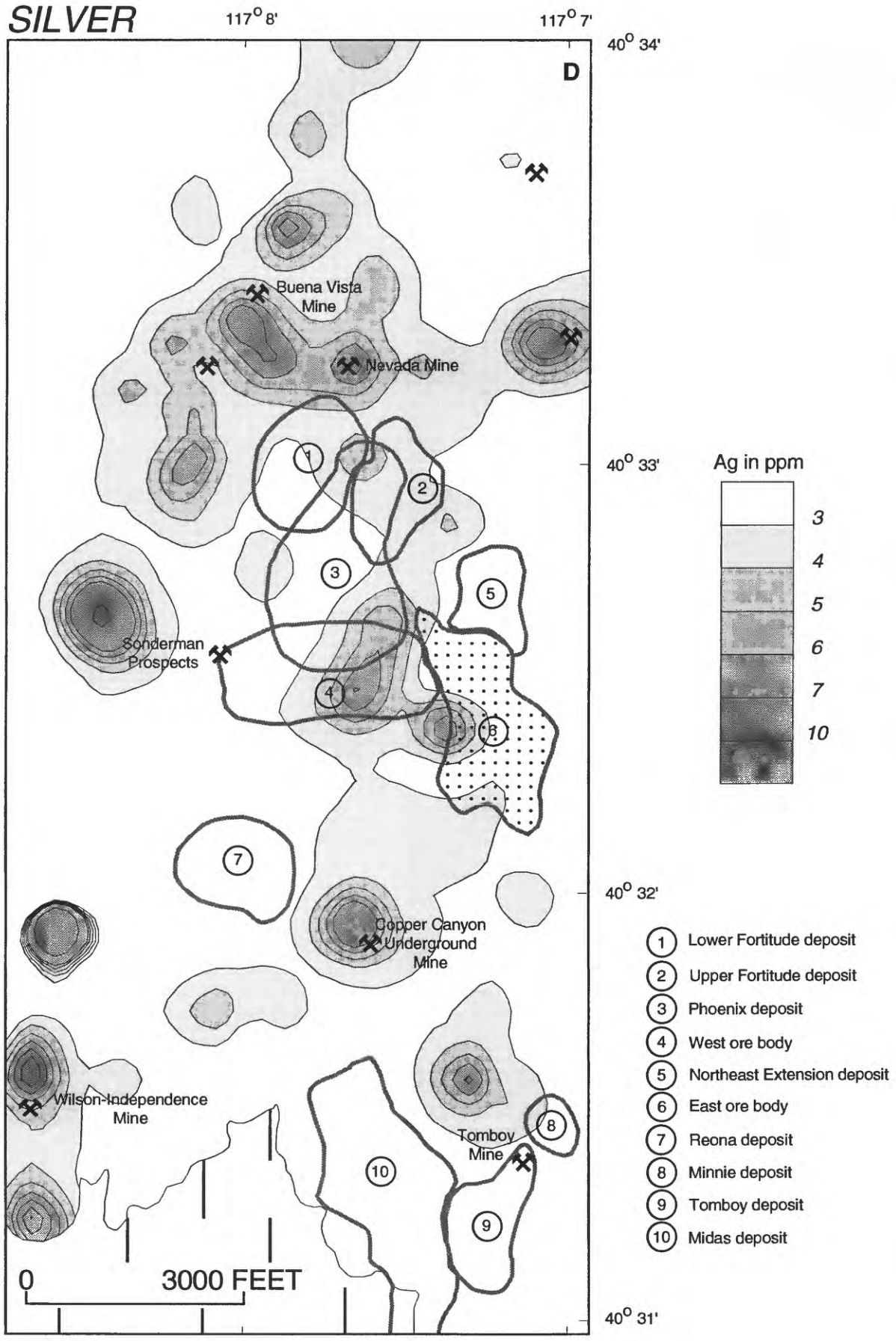

Figure 6. -- Continued.

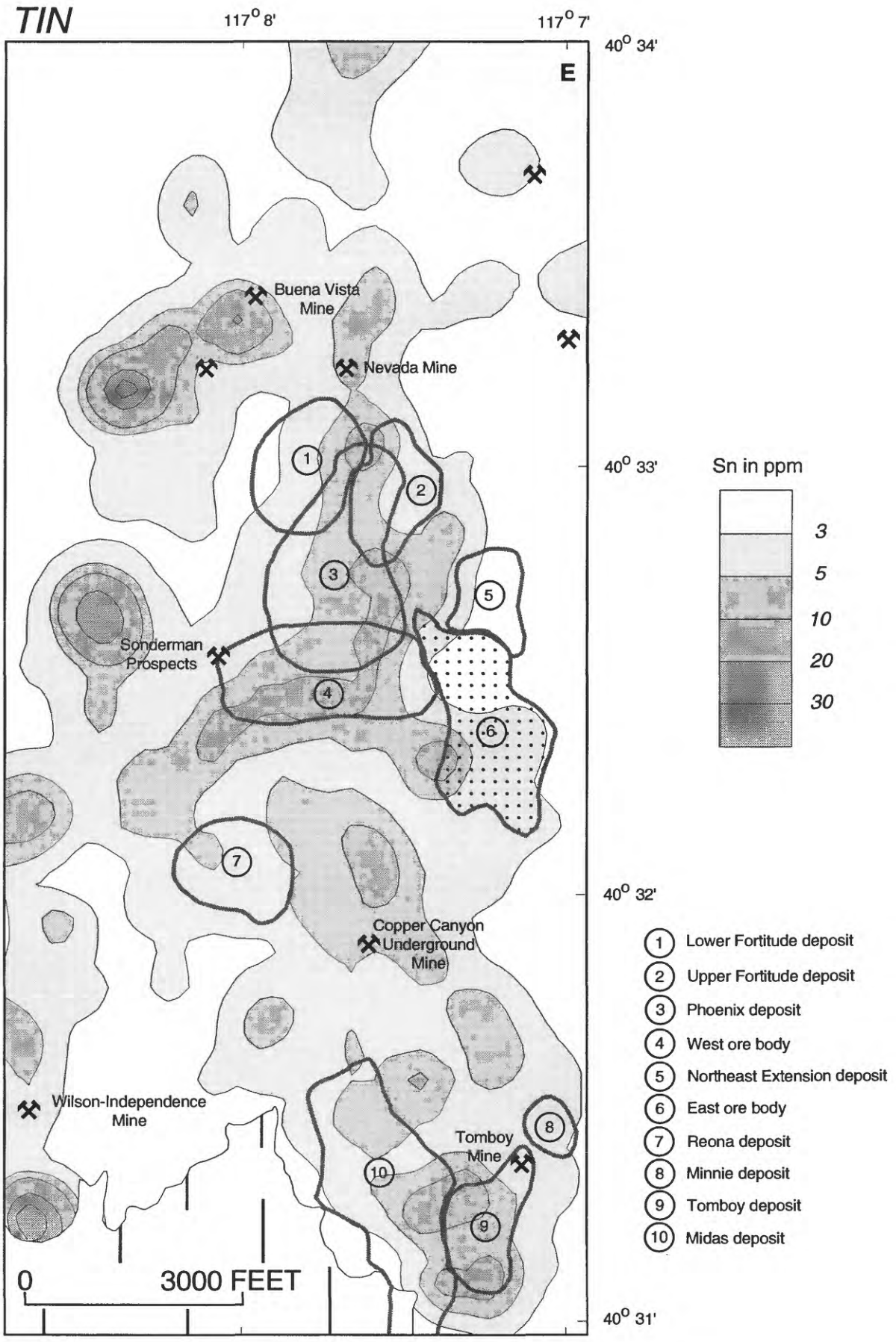

Figure 6. -- Continued.

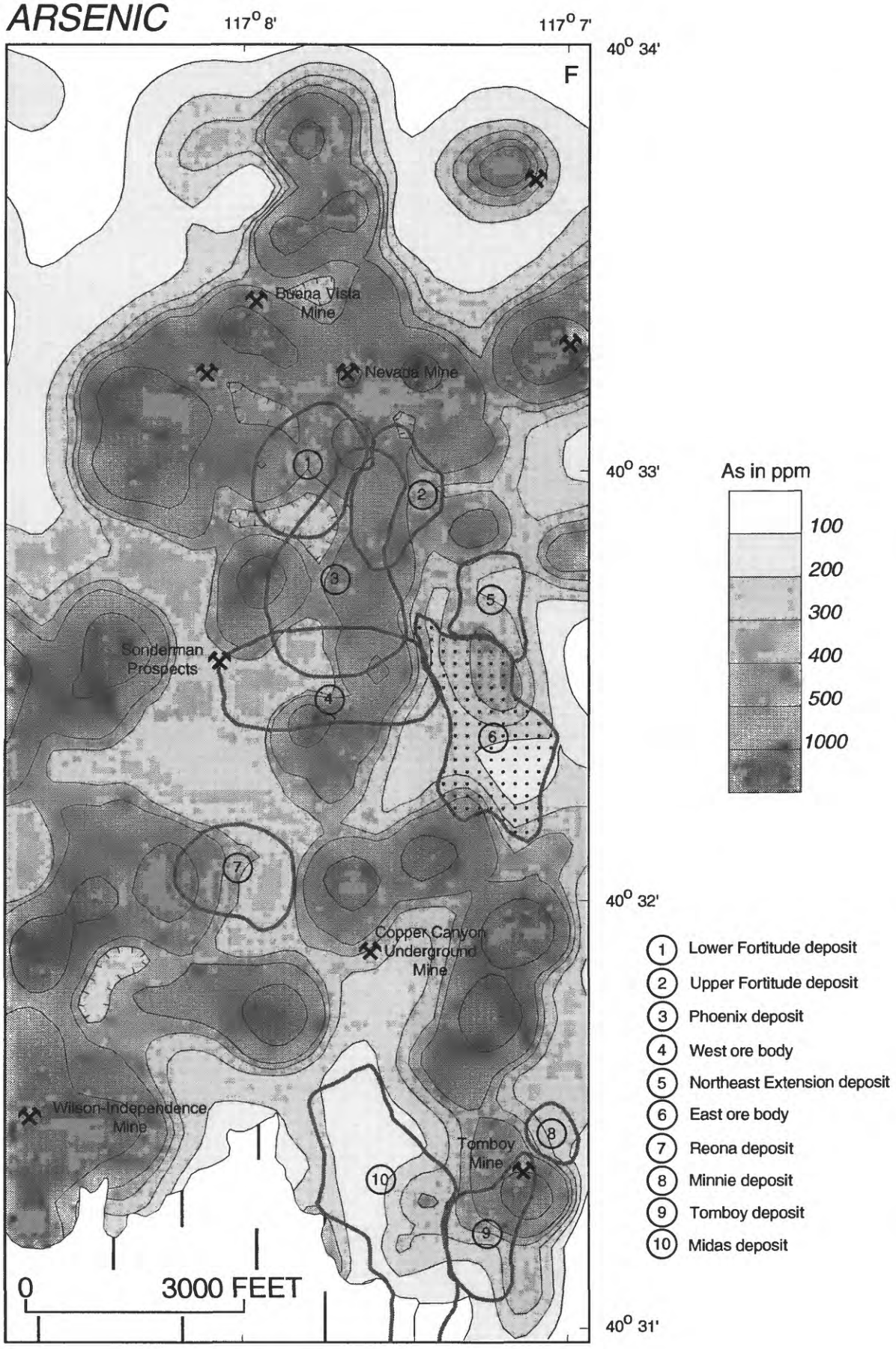

Figure 6. -- Continued.

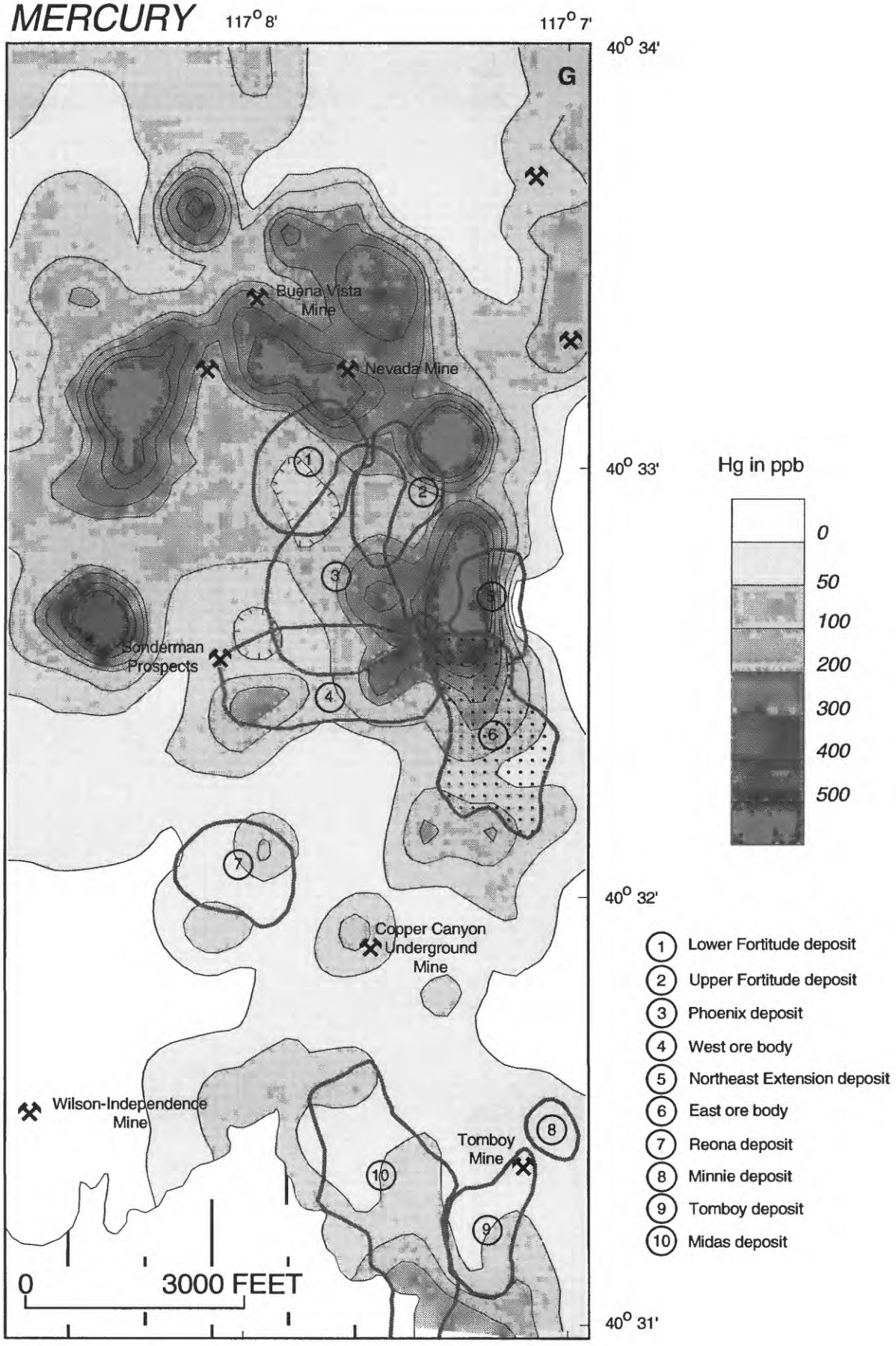

Figure 6. -- Continued.

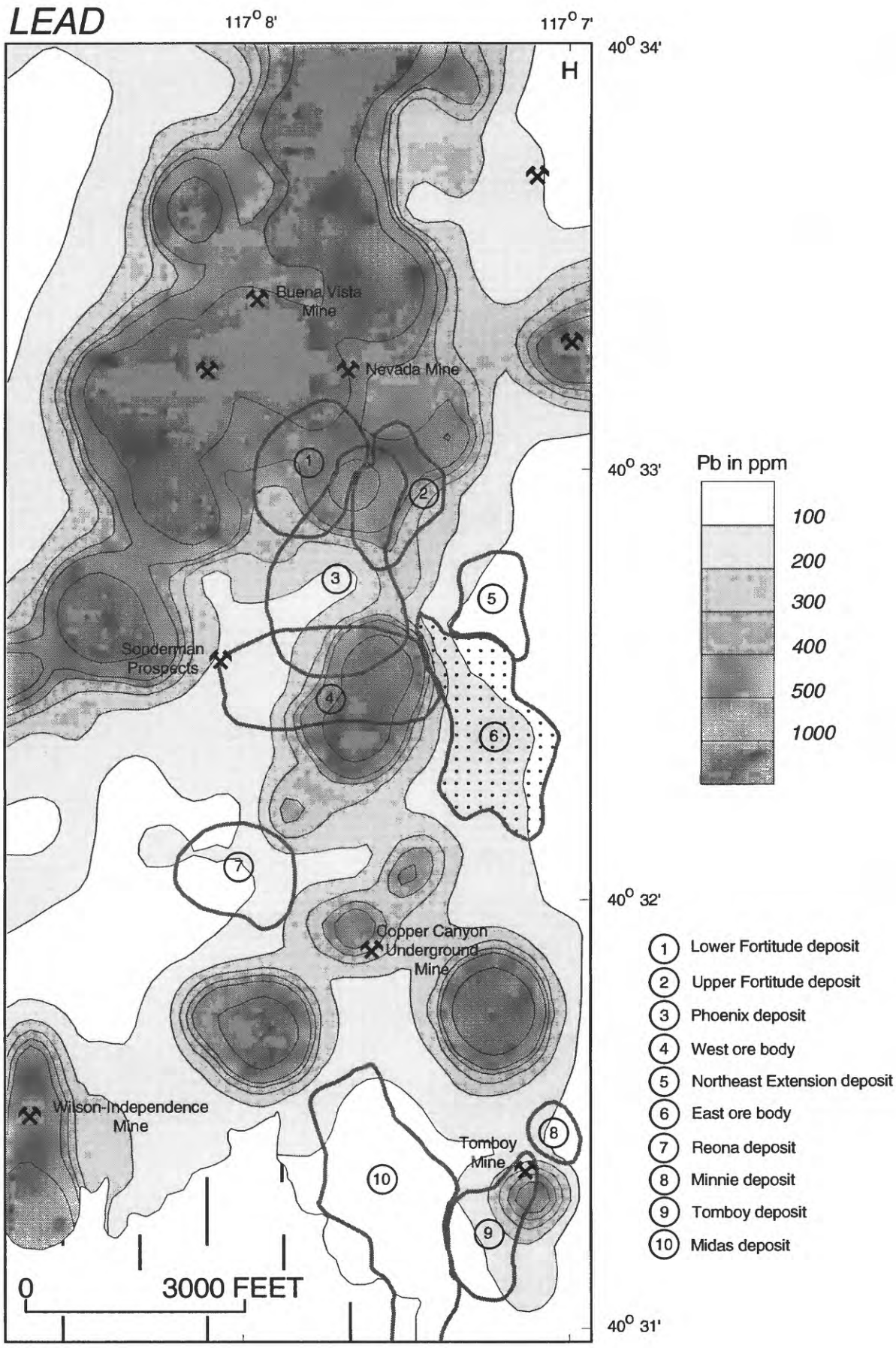

Figure 6. -- Continued.

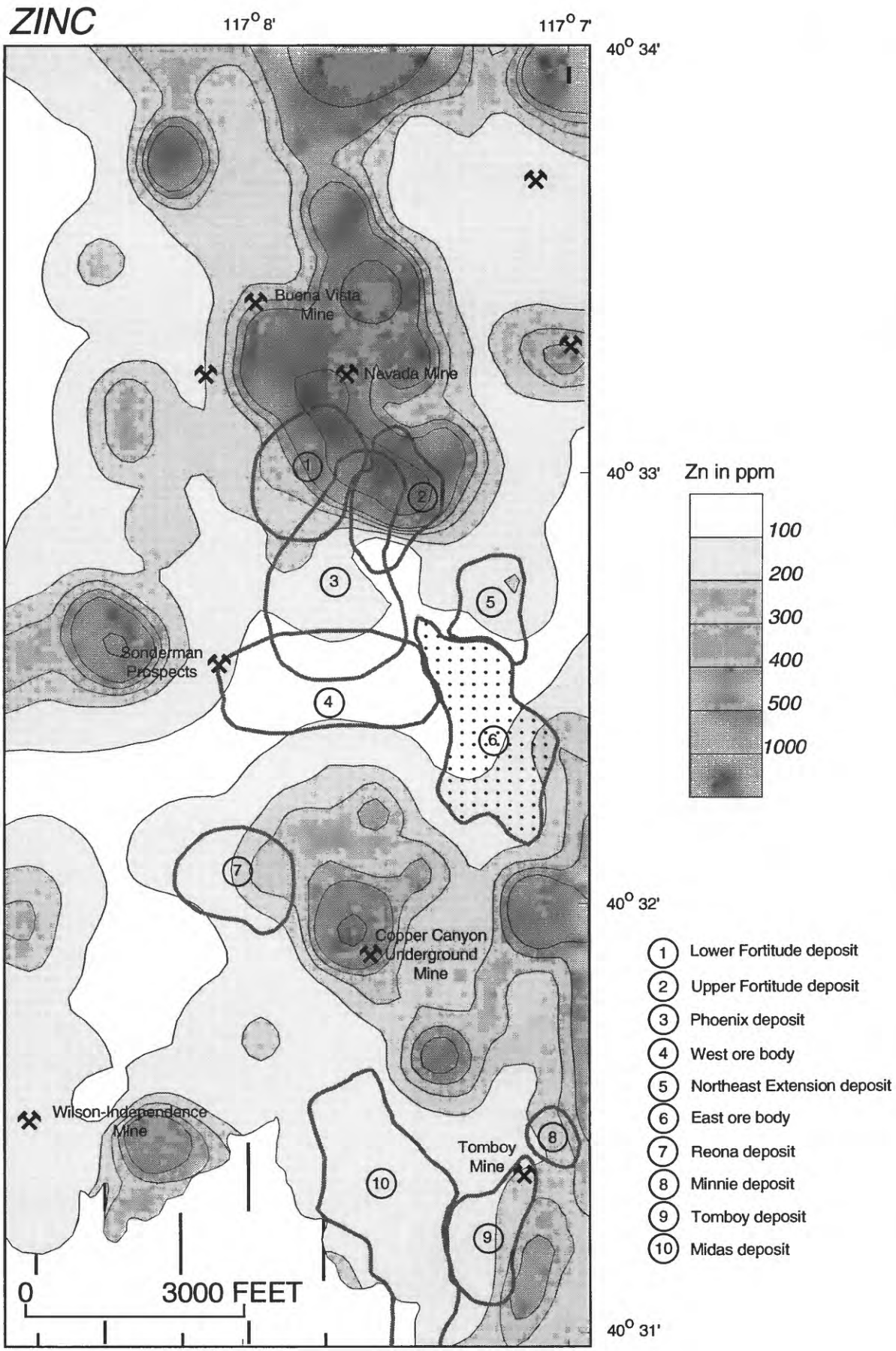

Figure 6. -- Continued.

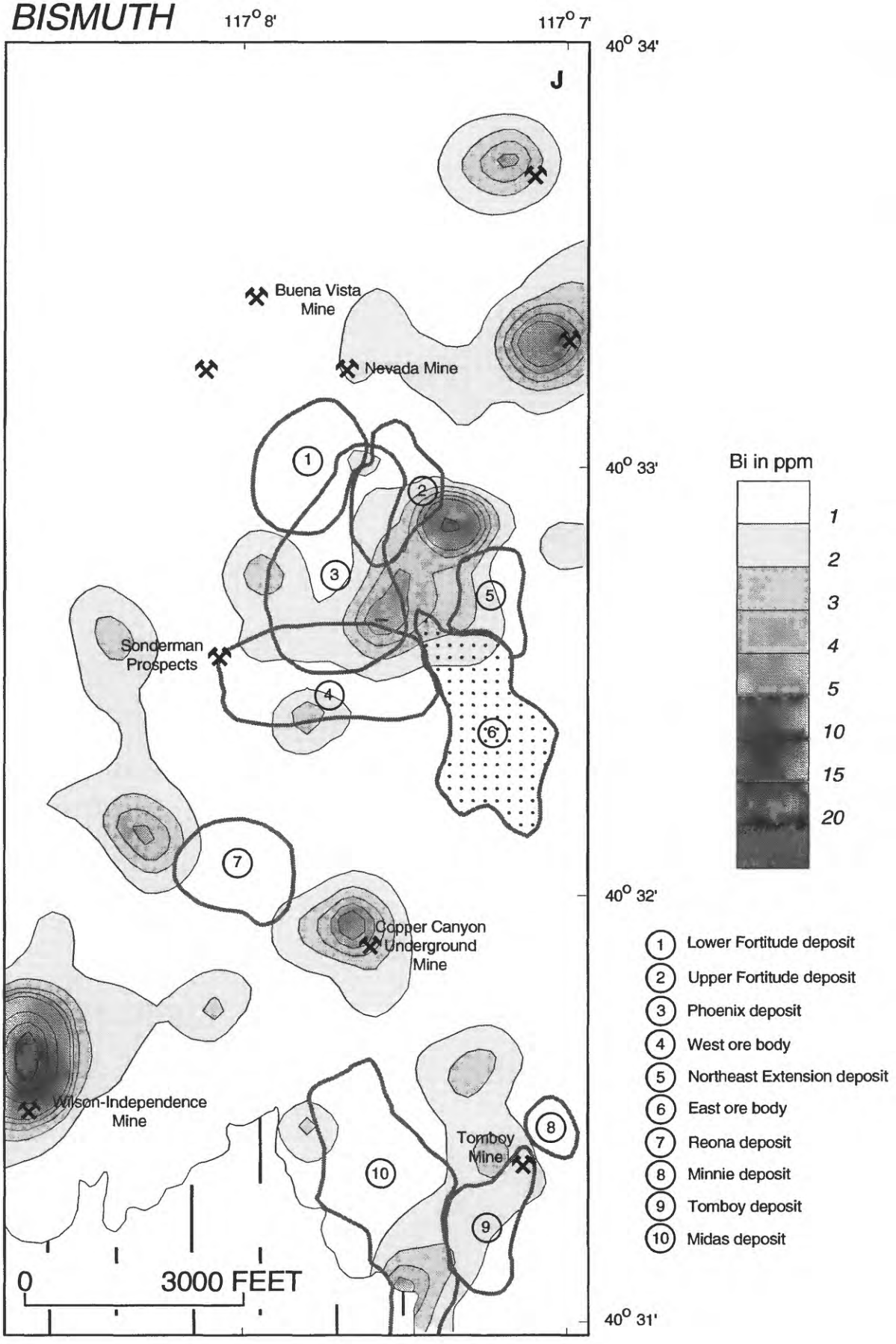

Figure 6. -- Continued.

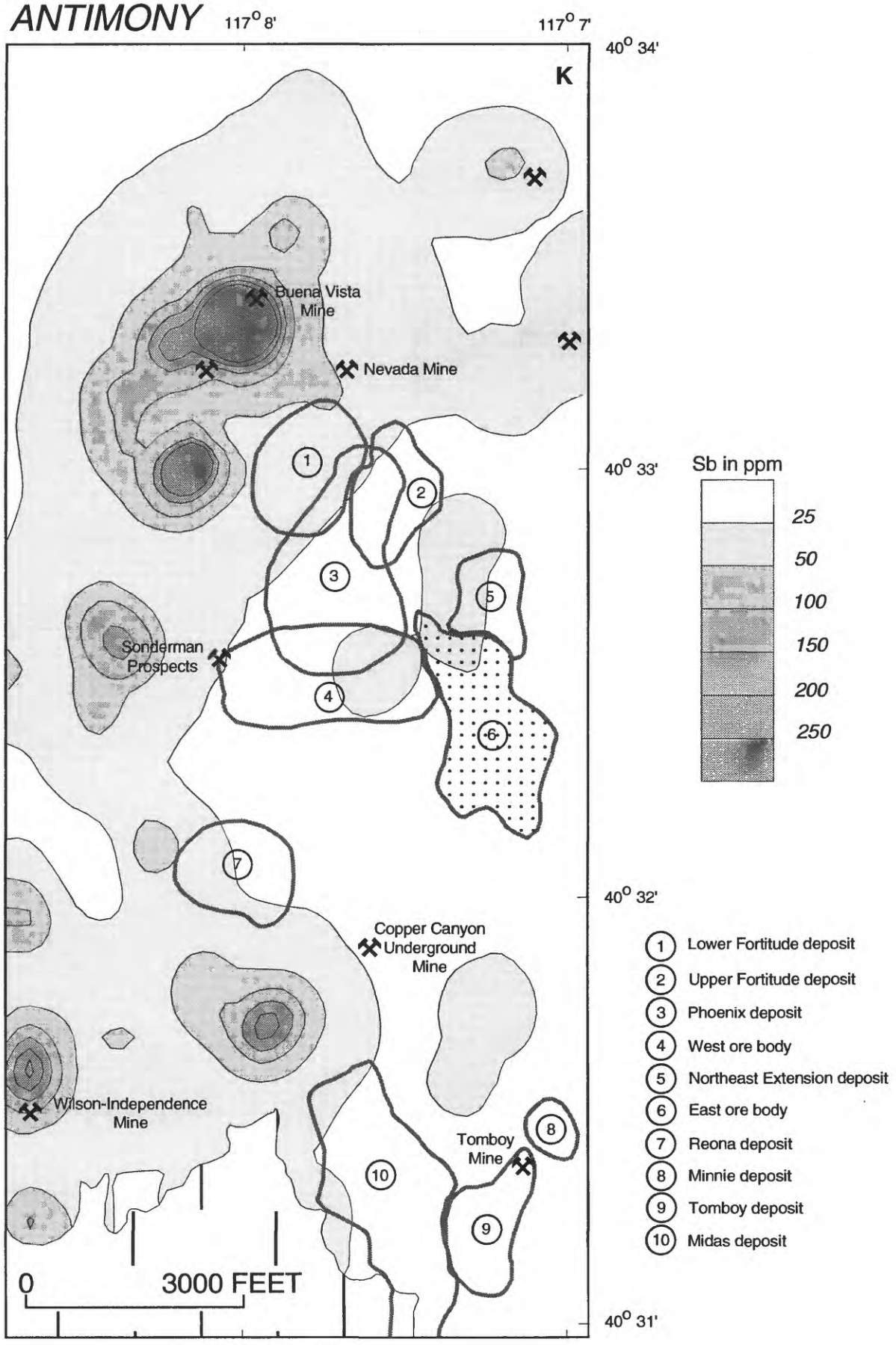

Figure 7.

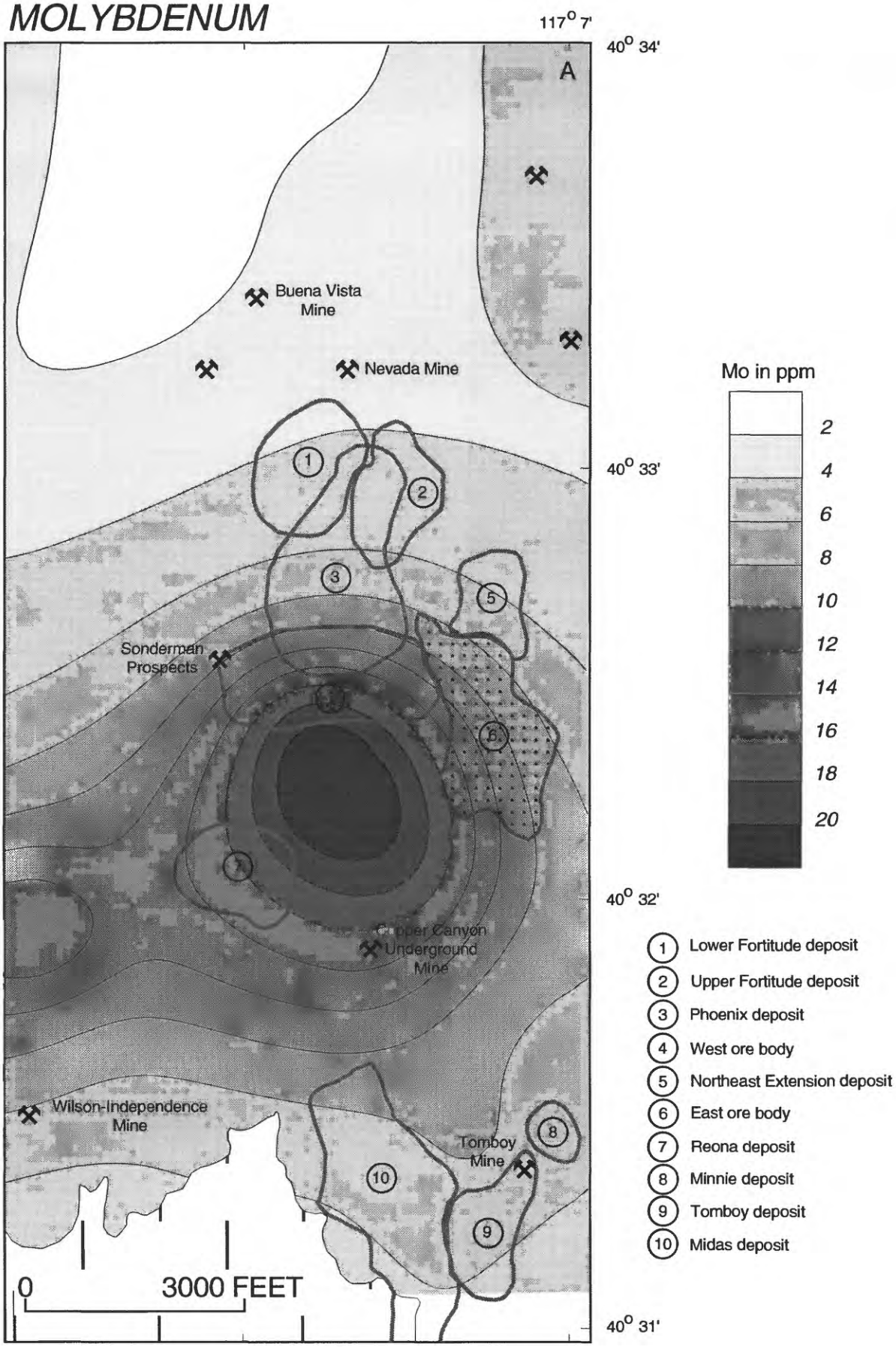
MOLYBDENUM
117° 7'
40° 34'
40° 33'
40° 32'
40° 31'
A
Buena Vista Mine
Nevada Mine
Sonderman Prospects
Upper Canyon Underground Mine
Wilson-Independence Mine
Tomboy Mine
0
3000 FEET
Mo in ppm
2
4
6
8
10
12
14
16
18
20
1 Lower Fortitude deposit
2 Upper Fortitude deposit
3 Phoenix deposit
4 West ore body
5 Northeast Extension deposit
6 East ore body
7 Reona deposit
8 Minnie deposit
9 Tomboy deposit
10 Midas deposit

Figure 7. -- Continued.

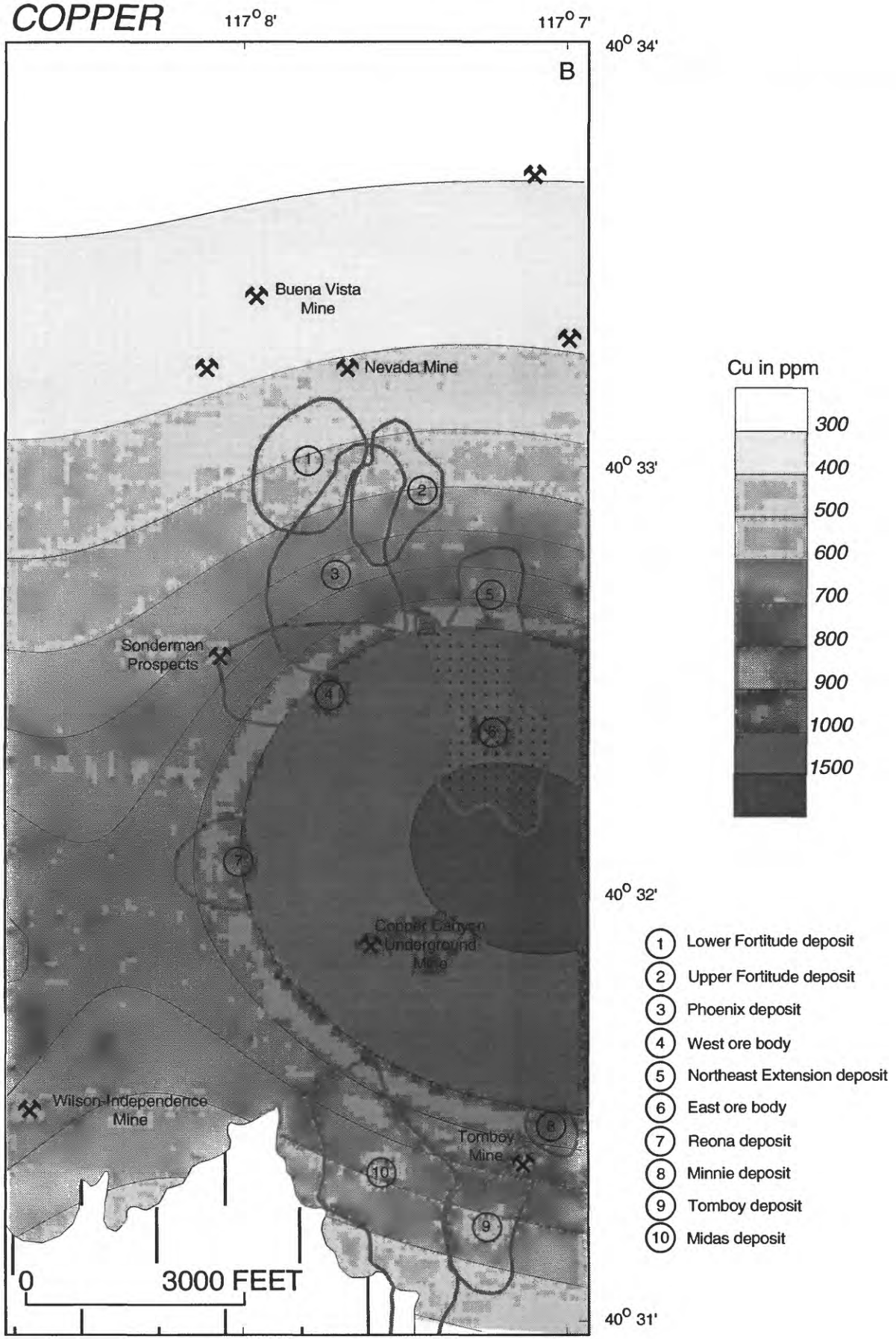

Figure 7. -- Continued.

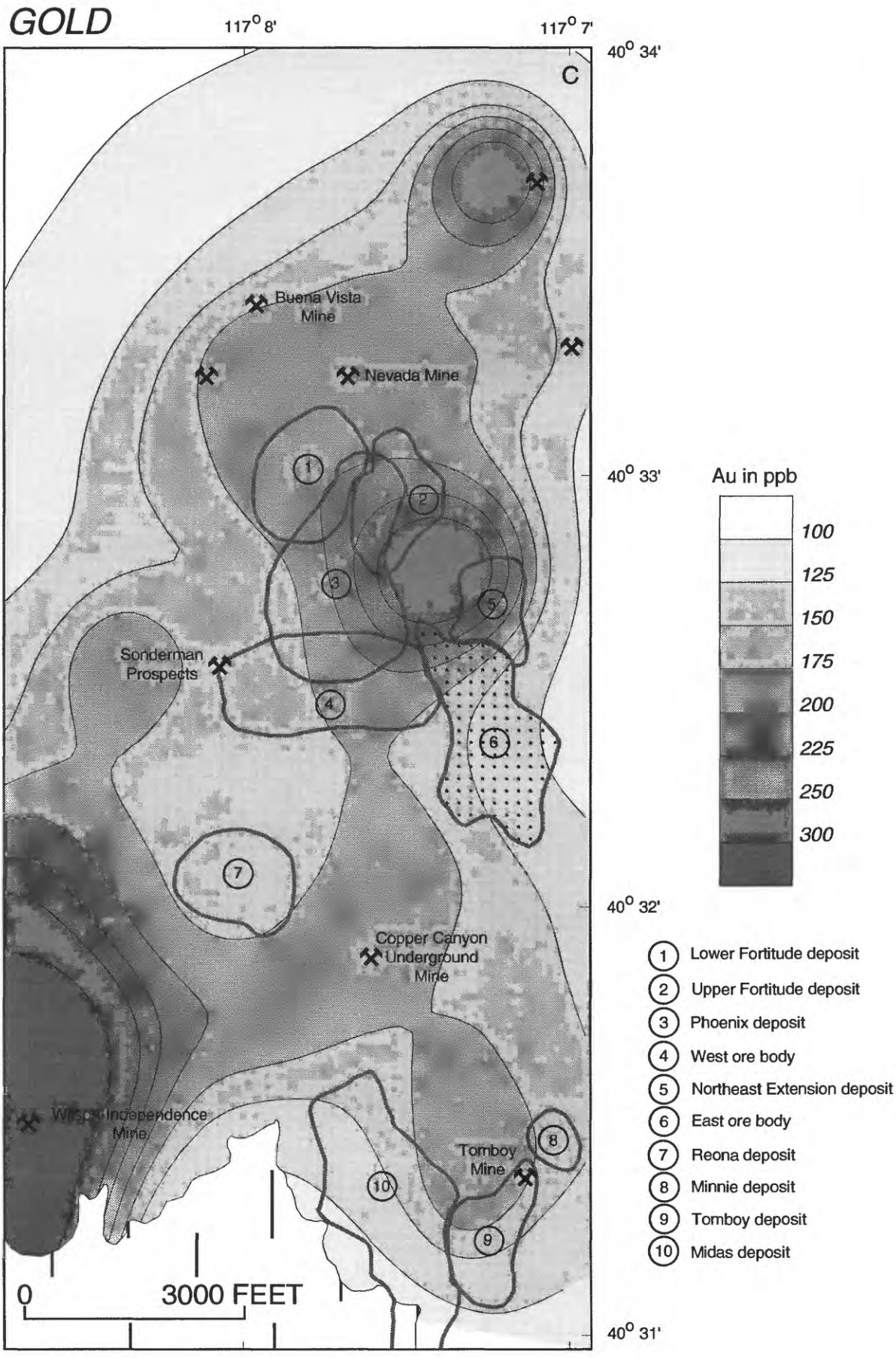

Figure 7. -- Continued.

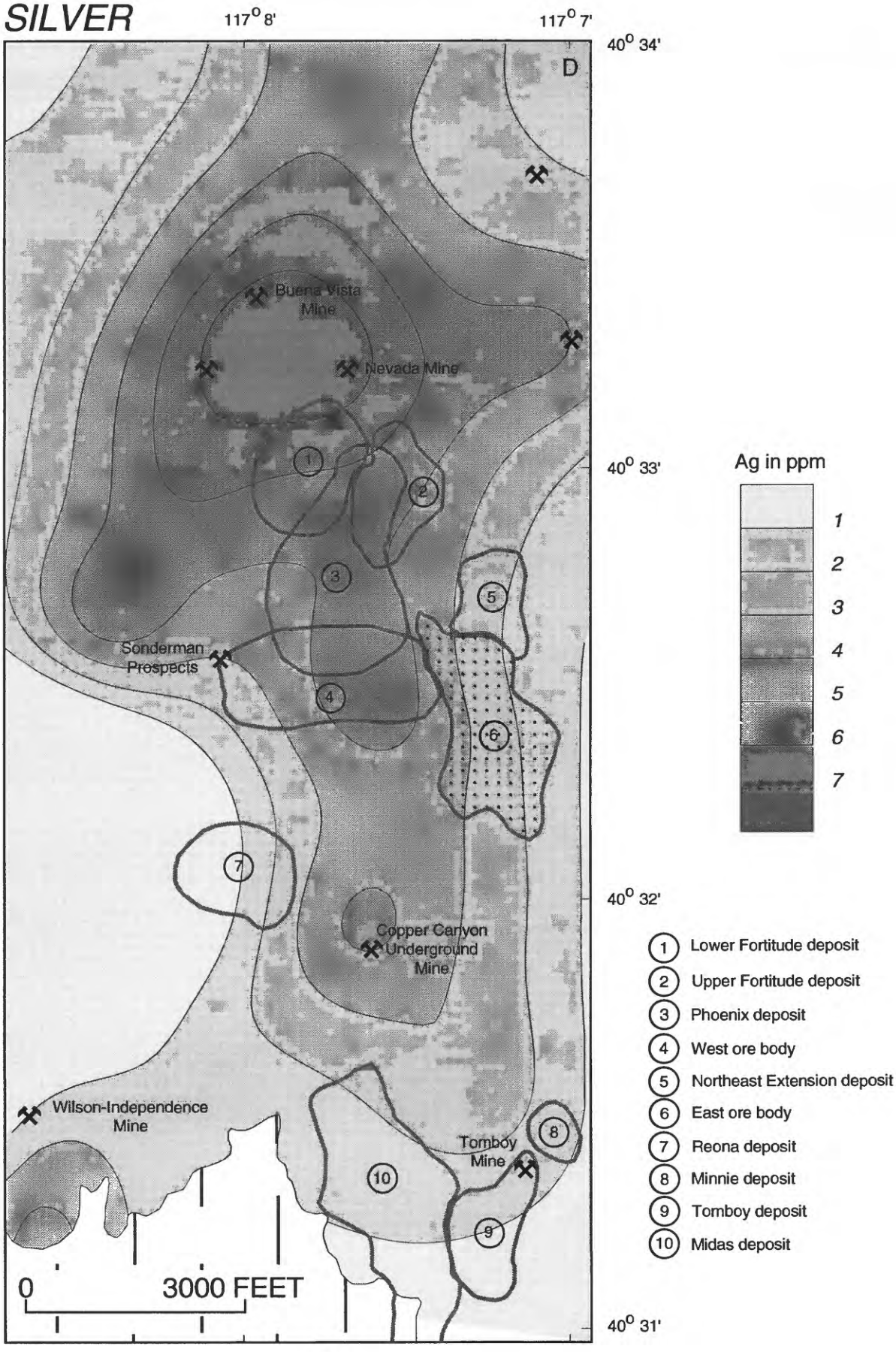

Figure 7. -- Continued.

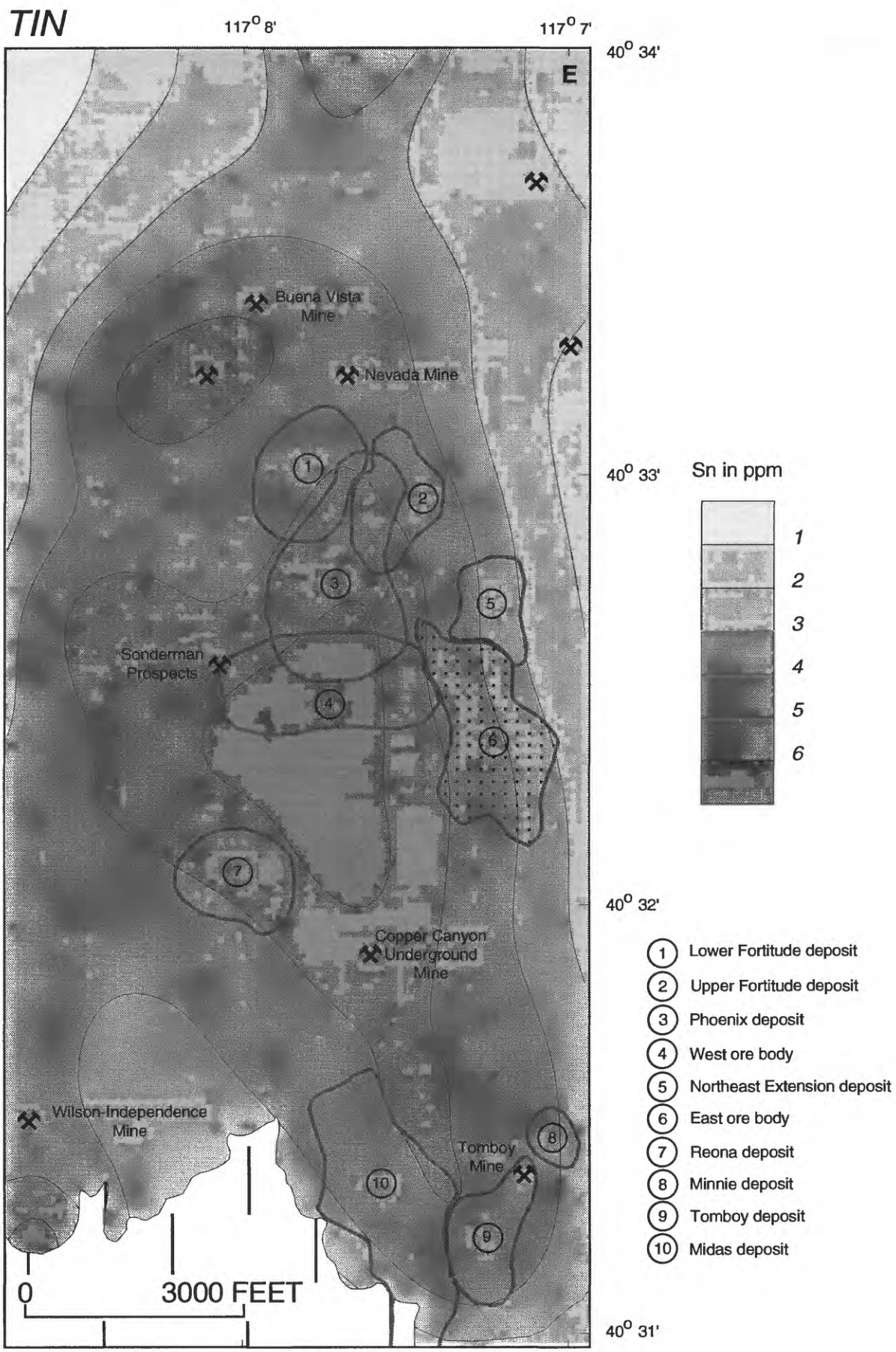

Figure 7. -- Continued.

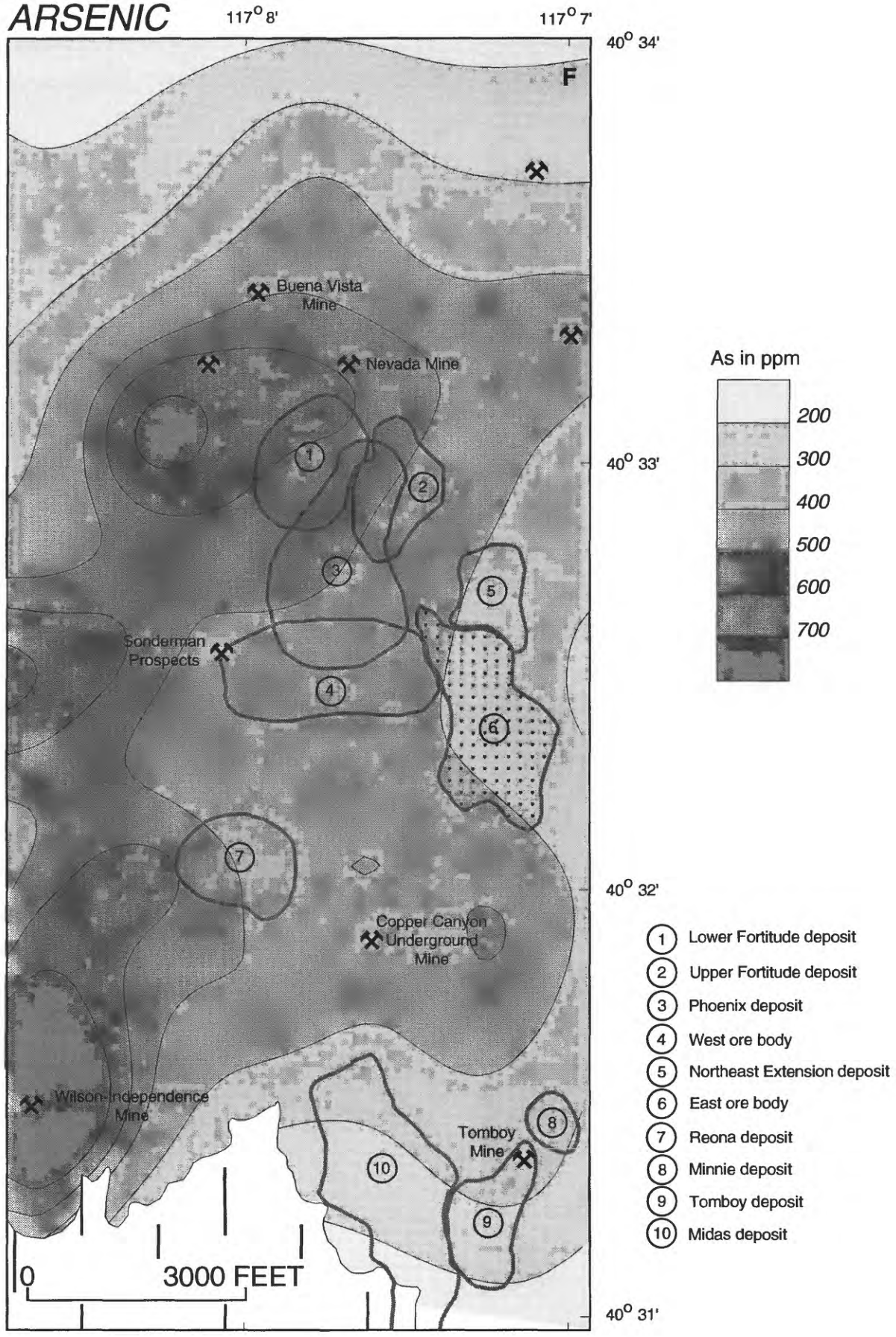

Figure 7. -- Continued.

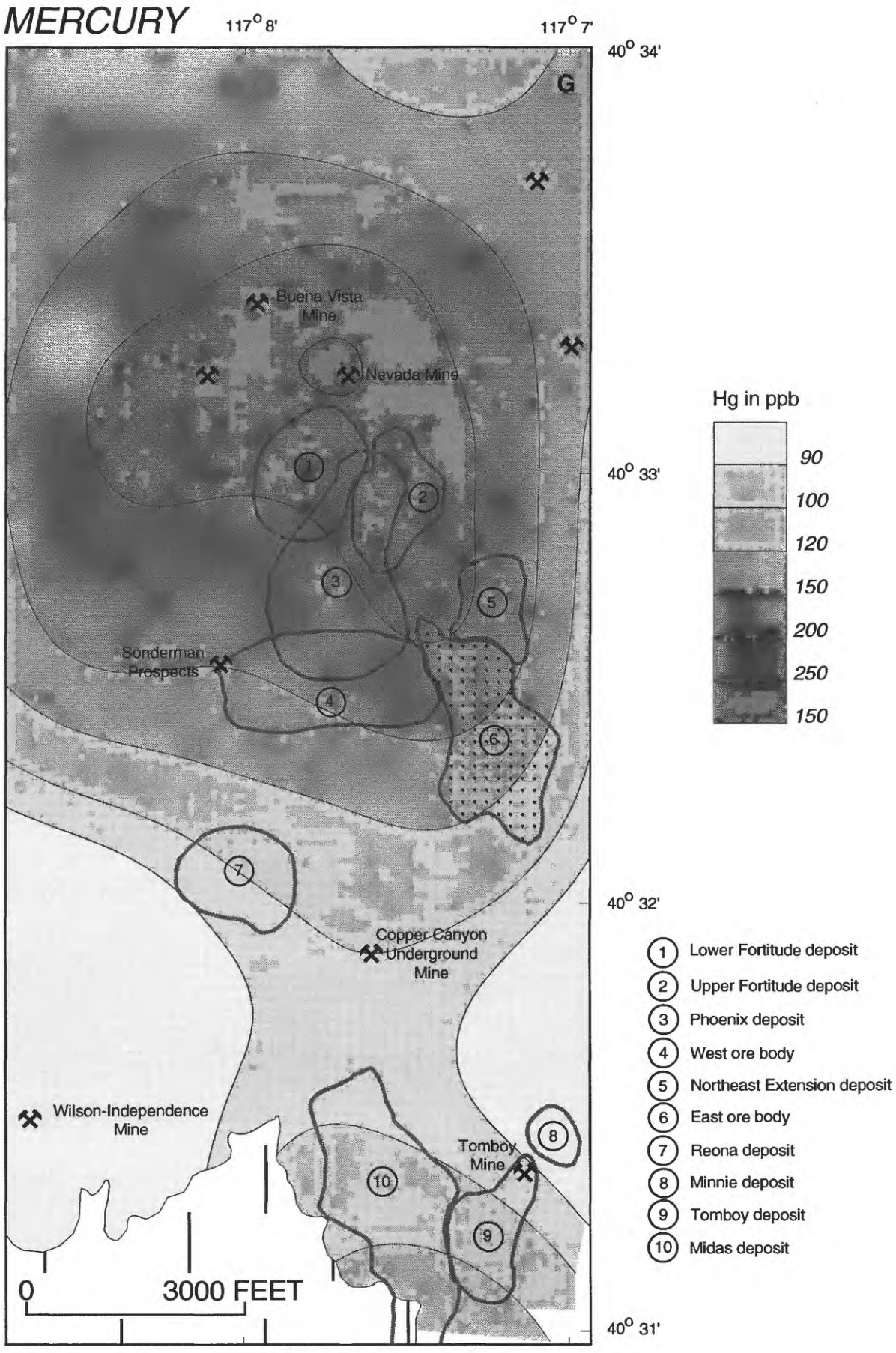

Figure 7. -- Continued.

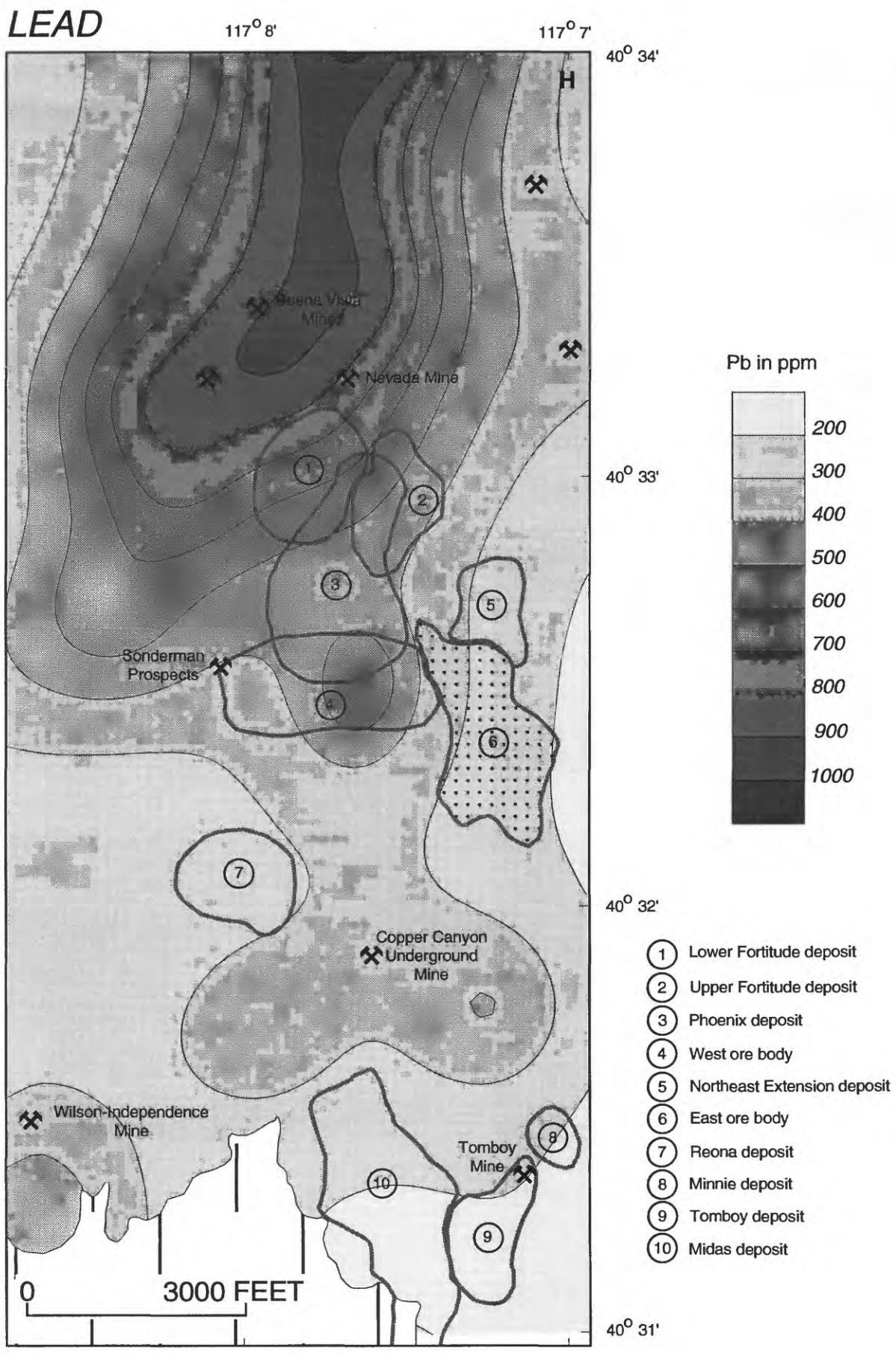

Figure 7. -- Continued.

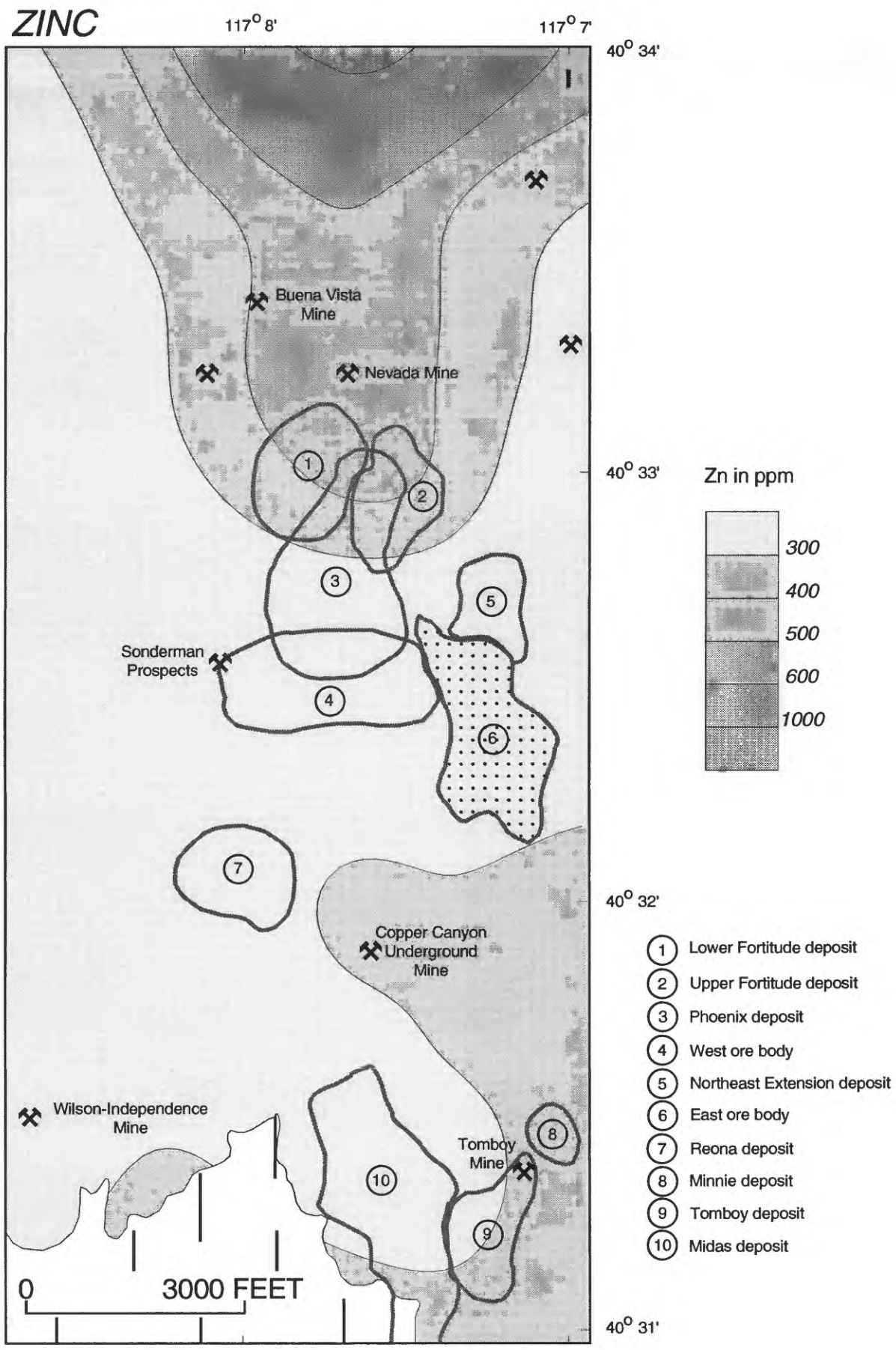

Figure 7. -- Continued.

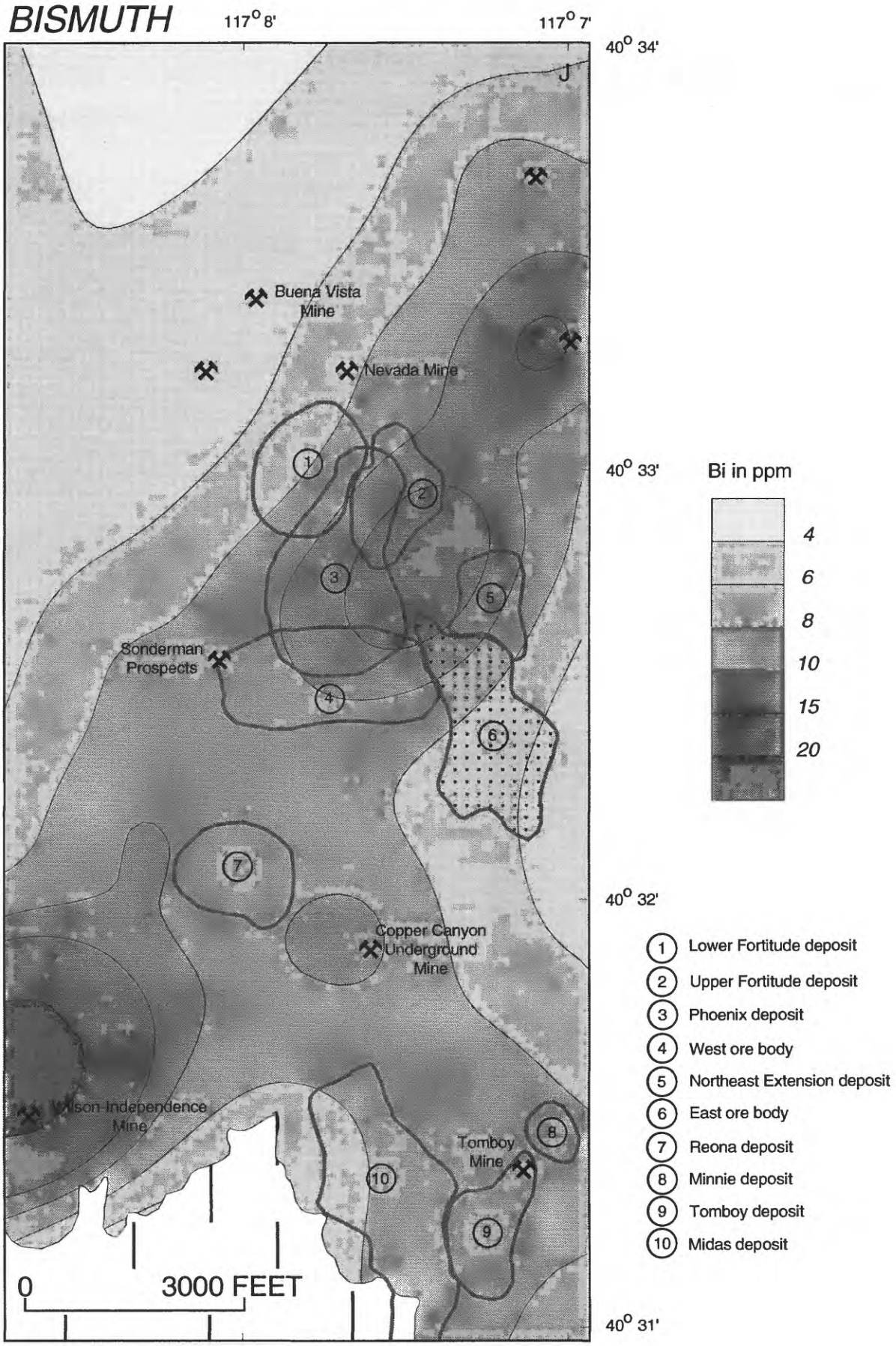

Figure 7. -- Continued.